NACA TN 4149

C.1

NATIONAL ADVISORY COMMITTEE FOR AERONAUTICS

TECHNICAL NOTE 4149

AN ANALYSIS OF THE TURBULENT BOUNDARY-LAYER CHARACTERISTICS ON A FLAT PLATE WITH DISTRIBUTED LIGHT-GAS INJECTION

By Morris W. Rubesin and Constantine C. Pappas

Ames Aeronautical Laboratory
Moffett Field, Calif.

LIBRARY COPY
FEB 20 1958
LANGLEY AERONAUTICAL LABORATORY
LIBRARY, NACA
LANGLEY FIELD, VIRGINIA

Washington
February 1958

NATIONAL ADVISORY COMMITTEE FOR AERONAUTICS

TECHNICAL NOTE 4149

AN ANALYSIS OF THE TURBULENT BOUNDARY-LAYER CHARACTERISTICS ON A FLAT PLATE WITH DISTRIBUTED LIGHT-GAS INJECTION

By Morris W. Rubesin and Constantine C. Pappas

SUMMARY

An exploratory analysis has been developed for the case of distributed injection of a foreign gas into a turbulent boundary layer in air on a flat plate. The work is divided into three parts: a derivation of the basic turbulent boundary-layer equations for a binary gas system; a derivation of modified Reynolds analogies between momentum, mass, and heat transfer for a binary gas system; and an evaluation of the effect of foreign gas injection on the skin friction and heat transfer of a nearly isothermal boundary layer by means of mixing length theory. Numerical results are presented for the injection of hydrogen and helium into the boundary layer for a temperature of 500° R. It has been found that the injection of a given mass of light gas is much more effective than the same mass of air in reducing skin friction and heat transfer on the flat plate. The same reductions are generally achieved with about 20 percent as much hydrogen and about 40 percent as much helium as in the case for air.

INTRODUCTION

The cooling of aircraft experiencing aerodynamic heating is becoming increasingly necessary as the speeds of contemplated aircraft become higher and higher. Even with the best of presently available high-temperature materials, the steady-state heating of external surfaces of aircraft flying at Mach numbers around 10 and higher will often require extensive cooling. High-level heating regions such as fuselage tips and wing leading edges require cooling at even lower Mach numbers. Cooling may even prove effective in transient heating systems, such as in ballistic missiles, because the heat absorbing ability of fluids used in cooling systems, such as water, hydrogen, or helium, greatly exceeds the heat absorbing ability of solid materials, without phase change, on a pound per pound basis.

Of the various cooling systems available, mass transfer systems in which the coolant is ultimately introduced into the boundary layer in contact with the aircraft surface appear to be more effective than the

more conventional internal cooling systems (ref. 1). The present paper is concerned with a transpiration cooling system in which the coolant passes through the surface it is protecting before entering the surrounding boundary layer. The boundary layer is considered to be turbulent. Analyses and experiments have been performed to determine the effect of distributed air transpiration through flat surfaces over which air flows in a turbulent boundary layer (refs. 2, 3, and 4). These investigations revealed that the transpiration process reduces both the skin friction and heat transfer associated with the boundary layer. These effects are qualitatively the same as the behavior of the laminar boundary layer under similar conditions at the surface (refs. 5 and 6). Now it is known (refs. 7 and 8) that injection of a light gas into the boundary layer at the surface is much more effective than the injection of air in reducing the skin friction of a laminar boundary layer on a flat plate.

It is the purpose of this study to determine if light gas injection affects the turbulent boundary layer in an analogous manner. The study is confined to the boundary layer on a flat plate and is divided into three parts:

(a) A derivation of the basic fully turbulent boundary-layer equations for a binary gas system, considering the diffusion only due to concentration gradients,

(b) An evaluation of modified Reynolds analogies between momentum, mass, and heat transfer for a binary gas system, and

(c) A determination of the effect of foreign gas injection on the skin friction and heat-transfer processes of a nearly isothermal turbulent boundary layer with the numerical results confined to the injection of helium and hydrogen. In this latter part, mixing length theory is employed even though it is known to be physically incorrect (ref. 9). The pragmatic viewpoint is taken. Mixing length theory has provided useful approximations in the past (refs. 2, 3, and 10), so it may be expected to do so in the present case as well.

SYMBOLS

c_f local skin-friction coefficient

c_p specific heat at constant pressure per unit mass

C constant of integration

D_{12} molecular diffusion coefficient for a binary mixture

F injection mass flow per unit area divided by the mass flow per unit area of stream just outside the boundary layer, $\frac{\rho_w v_w}{\rho_\infty u_\infty}$

g	symbol for exponential term in equation (68)
h	heat-transfer coefficient
i	enthalpy per unit mass
K	mixing length constant
m	symbol defined by equation (65)
M	molecular weight
n	symbol defined by equation (65)
p	pressure
Pr	Prandtl number of mixture, $\frac{\mu c_p}{\lambda}$
Pr^*	Prandtl number as defined by equation (43)
q_c	heat-transfer rate per unit area by molecular conduction
R_x	Reynolds number, $\frac{\rho_\infty u_\infty x}{\mu_\infty}$
R_y	Reynolds number, $\frac{\rho_\infty u_\infty y}{\mu_\infty}$
R_θ	Reynolds number, $\frac{\rho_\infty u_\infty \theta}{\mu_\infty}$
Sc	Schmidt number, $\frac{\mu}{\rho D_{12}}$
Sc'	turbulent Schmidt number, $\frac{\epsilon_v}{\rho \epsilon_d}$
St	Stanton number, $\frac{h}{\rho_\infty u_\infty c_{p_\infty}}$
T	temperature
u	mass velocity parallel to plate surface
$\tilde{u}$	dimensionless velocity, $\frac{u}{u_\infty}$
v	mass velocity normal to plate surface
x	distance along plate from leading edge
y	distance normal to plate surface

α,β defined by equations (81) and (82)

Γ defined by equation (44)

δ boundary-layer thickness per length of run

ϵ_d eddy diffusion coefficient

ϵ_ν eddy viscosity

ϵ_λ eddy thermal conductivity

ζ $\frac{F}{c_f/2}$

θ momentum thickness

λ molecular thermal conductivity

μ molecular viscosity

ρ density

σ temperature recovery factor

τ frictional shear stress

ω mass fraction of foreign gas

Superscripts

$\overline{(\ )}$ temporal mean value, see equation (8)

$'$ randomly fluctuating value

Subscripts

a condition at interface

a- condition at interface, on laminar sublayer side

a+ condition at interface, on turbulent side

w condition at surface of plate

∞ condition at outer edge of boundary layer

1 light gas

2 air

o zero injection condition

ANALYSIS

The analysis of this report is quite similar, in principle, to the analysis of reference 3. The main difference is that the basic equations used in the present analysis apply to a two-component mixture of gases, a foreign gas and air, rather than air alone. Air is treated as a single gas, having the mean properties of the mixture containing the following volume fractions: 0.78 N_2, 0.21 O_2, 0.01 A.

The turbulent boundary layer is considered to occur on a flat plate (i.e., $\partial p/\partial x = 0$) oriented parallel to the free stream. It is postulated to be composed of two regions: a laminar sublayer, where the transport of momentum, energy, and mass is controlled by molecular motion; and an outer turbulent region where the transport of properties is controlled by eddying motion. At the interface of these two regions, it is required that there be a continuity of velocity, temperature, shear, and mass and energy flux. The boundary layer is considered to be at steady state. Only the diffusion resulting from concentration gradients is included; the other diffusion processes are considered to be sufficiently small for the purposes of this report so that they can be neglected.

Basic Boundary-Layer Equations

When the usual boundary-layer order of magnitude argument is employed, the laminar transport equations for a bicomponent mixture on a flat plate can be derived from the equations for a nonreacting gas mixture of reference 11 (pp. 698, 498, and 516). The equations can be written as follows:

Continuity of mass

$$\frac{\partial}{\partial x}\rho u + \frac{\partial}{\partial y}\rho v = 0 \tag{1}$$

Conservation of momentum in x direction

$$\rho u \frac{\partial u}{\partial x} + \rho v \frac{\partial u}{\partial y} = \frac{\partial}{\partial y}\left(\mu \frac{\partial u}{\partial y}\right)$$

Conservation of momentum in y direction

$$\frac{\partial p}{\partial y} = 0 \tag{3}$$

Conservation of diffusing component

$$\rho u \frac{\partial \omega}{\partial x} + \rho v \frac{\partial \omega}{\partial y} = \frac{\partial}{\partial y}\left(\rho D_{12} \frac{\partial \omega}{\partial y}\right) \tag{4}$$

Conservation of thermal energy

$$\rho u \frac{\partial i}{\partial x} + \rho v \frac{\partial i}{\partial y} = \frac{\partial}{\partial y}\left[\lambda \frac{\partial T}{\partial y} + \rho D_{12} \frac{\partial \omega}{\partial y}(i_1 - i_2)\right] + \mu \left(\frac{\partial u}{\partial y}\right)^2 \tag{5}$$

An equation representing a conservation of total energy, $i + \frac{u^2}{2}$, can be obtained by combining equations (2) and (5). The resulting equation is

$$\rho u \frac{\partial}{\partial x}\left(i + \frac{u^2}{2}\right) + \rho v \frac{\partial}{\partial y}\left(i + \frac{u^2}{2}\right) = \frac{\partial}{\partial y}\left[\lambda \frac{\partial T}{\partial y} + \rho D_{12} \frac{\partial \omega}{\partial y}(i_1 - i_2) + u\mu \frac{\partial u}{\partial y}\right] \tag{6}$$

The corresponding equations for the turbulent portion of the boundary layer can be formed if it is assumed that the molecular transport terms, the right members of the above equations, are equal to zero. This implies that the left members represent an instantaneous convection of the corresponding properties and that molecular mechanisms are negligible. The instantaneous values of the dependent variables are then expressed as the sum of a term that is invariant with time and a term that varies rapidly with time in a random fashion. Thus, for example,

$$\left.\begin{aligned} u &= \overline{u} + u' \\ v &= \overline{v} + v' \\ \rho &= \overline{\rho} + \rho' \\ \omega &= \overline{\omega} + \omega' \\ i &= \overline{i} + i' \end{aligned}\right\} \tag{7}$$

The expressions (7) are then substituted into the left members of equations (1), (2), (4), and (6) which in turn have been set equal to zero. When averages of fluctuating quantities are defined as

$$\overline{A'} = \frac{1}{2\tau}\int_{-\tau}^{\tau} A'(\xi)\,d\xi \tag{8}$$

where τ is an interval of time sufficiently large to obtain a meaningful average, and when the following orders of magnitudes are applied,

$$\left.\begin{aligned}
&\overline{v},\ \overline{\rho'u'},\ \overline{\rho'v'},\ \text{etc.} \sim O(\delta)\\
&\overline{\rho'u'v'},\ \overline{\rho'u'u'},\ \text{etc.} \sim O(\delta^2)\\
&\overline{i},\ \overline{u},\ \overline{\rho},\ \overline{\omega},\ \frac{\partial}{\partial x} \sim O(1)\\
&\frac{\partial}{\partial y} \sim O(\delta^{-1}),\ \frac{\rho'(\tau) - \rho'(-\tau)}{2\tau} \to 0,\ \text{etc.}\\
&\omega',\ \rho',\ v',\ u',\ i' \ll 1
\end{aligned}\right\} \tag{9}$$

where $\delta \ll 1$ represents the boundary-layer thickness per unit of length of run, there result the following turbulent boundary-layer equations

$$\frac{\partial}{\partial x}\left(\overline{\rho}\overline{u}\right) + \frac{\partial}{\partial y}\left(\overline{\rho}\overline{v} + \overline{\rho'v'}\right) = 0 \tag{10}$$

$$\overline{\rho}\overline{u}\frac{\partial \overline{u}}{\partial x} + \left(\overline{\rho}\overline{v} + \overline{\rho'v'}\right)\frac{\partial \overline{u}}{\partial y} = \frac{\partial}{\partial y}\left(\epsilon_v \frac{\partial \overline{u}}{\partial y}\right) \tag{11}$$

$$\overline{\rho}\overline{u}\frac{\partial \overline{\omega}}{\partial x} + \left(\overline{\rho}\overline{v} + \overline{\rho'v'}\right)\frac{\partial \overline{\omega}}{\partial y} = \frac{\partial}{\partial y}\left(\overline{\rho}\epsilon_d \frac{\partial \overline{\omega}}{\partial y}\right) \tag{12}$$

$$\overline{\rho}\overline{u}\frac{\partial}{\partial x}\left(\overline{i} + \frac{\overline{u}^2}{2}\right) + \left(\overline{\rho}\overline{v} + \overline{\rho'v'}\right)\frac{\partial}{\partial y}\left(\overline{i} + \frac{\overline{u}^2}{2}\right) = \frac{\partial}{\partial y}\left[\epsilon_\lambda \frac{\partial \overline{T}}{\partial y} + \overline{\rho}\epsilon_d \frac{\partial \overline{\omega}}{\partial y}\left(\overline{i}_1 - \overline{i}_2\right) + \overline{u}\epsilon_v \frac{\partial \overline{u}}{\partial y}\right] \tag{13}$$

where

$$\left.\begin{aligned}
\epsilon_v &= -\overline{\rho}\,\frac{\overline{u'v'}}{\partial \overline{u}/\partial y}\\
\epsilon_\lambda &= -\overline{\rho}\overline{c_p}\,\frac{\overline{v'T'}}{\partial \overline{T}/\partial y}\\
\epsilon_d &= -\,\frac{\overline{v'\omega'}}{\partial \overline{\omega}/\partial y}
\end{aligned}\right\} \tag{14}$$

Boundary Conditions

The boundary conditions imposed on the above equations are at $y = 0$:

$$\left.\begin{aligned} u &= 0 \\ T &= T_w \\ \omega &= \omega_w \\ i_{1_w} &= i_1(T_w) \\ i_{2_w} &= i_2(T_w) \end{aligned}\right\} \tag{15}$$

as $y \rightarrow \infty$:

$$\left.\begin{aligned} u &= u_\infty \\ T &= T_\infty \\ \omega &= 0 \\ i_{1_\infty} &= i_1(T_\infty) \\ i_{2_\infty} &= i_2(T_\infty) \end{aligned}\right\} \tag{16}$$

The boundary condition $\omega = \omega_w$ at $y = 0$ (eq.(15)) requires some explanation. Only in the case of surface evaporation can the value of ω_w be prescribed, since then the partial pressure of a vapor over a liquid is a function of the liquid temperature. If the light gas is injected into the boundary layer, the concentration at the surface, ω_w, will depend on the diffusion rate through the boundary layer as well as the injection rate. This dependence can be seen from the following arguments. The average mass flow per unit area at the surface can be written as

$$\rho_w v_w = (\rho_1 v_1)_w + (\rho_2 v_2)_w \tag{17}$$

At the steady-state conditions, after air has diffused into the surface and established an equilibrium concentration, there is no more net air flow through the surface. Therefore $(v_2)_w = 0$ and

$$\rho_w v_w = (\rho_1 v_1)_w \tag{18}$$

Equation (18) can be rewritten as

$$(\rho_{1_w} + \rho_{2_w}) v_w = \rho_{1_w} v_{1_w}$$

since $\rho = \rho_1 + \rho_2$, and dividing through by ρ_w results in

$$\left[\left(\frac{\rho_1}{\rho}\right)_w + \left(\frac{\rho_2}{\rho}\right)_w\right]v_w = \left(\frac{\rho_1}{\rho}\right)_w v_{1_w}$$

Since $\left(\frac{\rho_2}{\rho}\right)_w = 1 - \left(\frac{\rho_1}{\rho}\right)_w$ by definition, and $\omega = \frac{\rho_1}{\rho}$

$$(1 - \omega_w)v_w = \omega_w(v_{1_w} - v_w) \tag{19}$$

Now $v_{1_w} - v_w$ defines the diffusion velocity of the injected gas and is represented by

$$\omega_w(v_{1_w} - v_w) = -\left(D_{12}\frac{d\omega}{dy}\right)_w$$

Therefore

$$(1 - \omega_w)v_w\rho_w = -\rho_w D_{12_w}\left(\frac{d\omega}{dy}\right)_w \tag{20}$$

Equation (20), then, is a more useful definition for the surface concentration, ω_w, than (15) for a nonevaporative system.

The above system of equations, together with the boundary conditions, is intractable because of its complexity and a lack of knowledge about the functional dependence of the eddy coefficients. At present, then, approximate methods are necessary.

Simplified Boundary-Layer Equations

Experience with the theory for turbulent boundary layers on flat plates (e.g., refs. 2 and 3) has shown that for practical purposes, variations of dependent variables at a fixed value of x can be found by treating the boundary-layer equations as total differential equations in y alone, the terms containing differentiation with respect to x being neglected. In this process, ultimately, variations in the x direction are introduced by the x variation of the shear and heat transfer at the wall. This is the technique employed in the present analysis also. The simplified boundary-layer equations can be written for the laminar sublayer as

$$\frac{d}{dy}(\rho v) = 0 \qquad \text{or} \qquad \rho v = \rho_w v_w \tag{21}$$

and

$$\rho_w v_w \frac{du}{dy} = \frac{d}{dy}\left(\mu \frac{du}{dy}\right) \tag{22}$$

$$\rho_w v_w \frac{d\omega}{dy} = \frac{d}{dy}\left(\rho D_{12} \frac{d\omega}{dy}\right) \tag{23}$$

$$\rho_w v_w \frac{d}{dy}\left(i + \frac{u^2}{2}\right) = \frac{d}{dy}\left[\lambda \frac{dT}{dy} + \rho D_{12} \frac{d\omega}{dy}(i_1 - i_2) + u\mu \frac{du}{dy}\right] \tag{24}$$

The corresponding equations for the turbulent portion of the boundary layer can be written as

$$\frac{d}{dy}\left(\bar{\rho}\bar{v} + \overline{\rho' v'}\right) = 0 \qquad \text{or} \qquad \bar{\rho}\bar{v} + \overline{\rho' v'} = \text{const.} = \rho_w v_w \tag{25}$$

and

$$\rho_w v_w \frac{du}{dy} = \frac{d}{dy}\left(\epsilon_v \frac{du}{dy}\right) \tag{26}$$

$$\rho_w v_w \frac{d\omega}{dy} = \frac{d}{dy}\left(\rho \epsilon_d \frac{d\omega}{dy}\right) \tag{27}$$

$$\rho_w v_w \frac{d}{dy}\left(i + \frac{u^2}{2}\right) = \frac{d}{dy}\left[\epsilon_\lambda \frac{dT}{dy} + \rho \epsilon_d \frac{d\omega}{dy}(i_1 - i_2) + u\epsilon_v \frac{du}{dy}\right] \tag{28}$$

The superscript bars are no longer needed for clarity.

Derivation of Reynolds Analogies

Before one can solve for the skin friction and heat transfer associated with the boundary layer, it is necessary to relate the local temperature and concentration with the local velocity. This facilitates later integrations and also permits analogies between momentum, mass, and heat transfer.

Analogy between skin friction and diffusion.- In the sublayer, the relation between momentum and mass transfer can be determined from equations (22) and (23). If each is integrated with respect to y and the boundary conditions at $y = 0$ are imposed, there results

$$\rho_w v_w u + \tau_w = \mu \frac{du}{dy} \tag{29}$$

and

$$\rho_w v_w(\omega - 1) = \rho D_{12} \frac{d\omega}{dy} \tag{30}$$

If the right and left members of equation (30) are divided by the corresponding members of equation (29), and the resultant equation integrated employing

$$Sc = \frac{\mu}{\rho D_{12}} = \text{const.} \tag{31}$$

for simplicity, there results

$$\frac{\omega - 1}{\omega_a - 1} = \left[\frac{F\tilde{u} + (c_f/2)}{F\tilde{u}_a + (c_f/2)}\right]^{Sc} \tag{32}$$

In equation (32) the arbitrary constant of integration was evaluated at the interface and the variables were made dimensionless.

In the outer turbulent portion, equations (26) and (27) are integrated with respect to y and subjected to the requirements that the velocity, concentration, shear, and diffusion rate be continuous across the interface, namely

$$\left.\begin{aligned} u_{a-} = u_{a+}\ , \quad \left(\mu \frac{du}{dy}\right)_{a-} &= \left(\epsilon_v \frac{du}{dy}\right)_{a+} \\ \omega_{a-} = \omega_{a+}\ , \left(\rho D_{12} \frac{d\omega}{dy}\right)_{a-} &= \left(\rho \epsilon_d \frac{d\omega}{dy}\right)_{a+} \end{aligned}\right\} \tag{33}$$

There results

$$\rho_w v_w u + \tau_w = \epsilon_v \frac{du}{dy} \tag{34}$$

$$\rho_w v_w(\omega - 1) = \rho \epsilon_d \frac{d\omega}{dy} \tag{35}$$

Again, as in the sublayer, dividing equation (35) by equation (34), performing the integration with

$$Sc' = \frac{\epsilon_v}{\rho\epsilon_d} = \text{const.} \tag{36}$$

and applying the boundary conditions at $y \longrightarrow \infty$ yields

$$1 - \omega = \left[\frac{F\tilde{u} + (c_f/2)}{F + (c_f/2)}\right]^{Sc'} \tag{37}$$

When the value of ω_a at the interface is eliminated between equations (32) and (37) and the wall condition is evaluated, there results

$$1 - \omega_w = \frac{(c_f/2)^{Sc}\left[F\tilde{u}_a + (c_f/2)\right]^{Sc' - Sc}}{\left[F + (c_f/2)\right]^{Sc'}} \tag{38}$$

which represents an analogy between diffusion and momentum transfer.

Analogy between skin friction and heat transfer.- The derivation of the relationship between heat and momentum transfer is more complex than the work of the preceding section because the effect of the simultaneous mass transfer must be isolated. When the Prandtl and Schmidt numbers (laminar or turbulent) are equal, it is possible to consider total enthalpy only; however, when they differ, it is necessary to consider both temperature and concentration. The assumption of equal Prandtl and Schmidt numbers is made in the turbulent portion of the boundary layer.

In the laminar sublayer integration of equation (24) together with incorporation of equation (30) results in

$$\rho_w v_w\left(i + \frac{u^2}{2}\right) = \lambda \frac{dT}{dy} + \rho_w v_w(\omega - 1)(i_1 - i_2) + \mu u \frac{du}{dy} + C \tag{39}$$

Now, the enthalpy term on the left, although largely dependent on T, is also dependent on the concentration ω. The members on the right contain terms which are dependent on temperature alone, dT/dy and $i_1 - i_2$. To make the terms of the equation more consistent, the enthalpy term i of the left member is expanded as

$$i = \omega i_1 + (1 - \omega) i_2$$

and equation (39) becomes

$$\rho_w v_w\left(i_1 - i_{1_w} + \frac{u^2}{2}\right) - q_{c_w} = \lambda \frac{dT}{dy} + u\mu \frac{du}{dy} \tag{40}$$

where the arbitrary constant evaluated at $y = 0$, is

$$C = \rho_w v_w i_{1_w} + q_{c_w} \tag{41}$$

The independent variable in equation (40) is changed from y to u by dividing corresponding members of equation (40) by those of equation (29). In addition, the first term on the right of equation (40) is multiplied and divided by c_{p_1}. There results

$$\frac{\rho_w v_w\left[i_1 - i_{1_w} + (u^2/2)\right] - q_{c_w}}{\rho_w v_w u + \tau_w} = \frac{\lambda}{\mu c_{p_1}} \frac{di_1}{du} + u \tag{42}$$

Note that the condition of the equality of temperature of the individual components and the mixture is employed here. It is also to be noted that a peculiar type of Prandtl number appears in equation (42), where the normal term c_p is replaced by c_{p_1}. If, for mathematical simplicity,

$$Pr^* = \frac{\mu c_{p_1}}{\lambda} \tag{43}$$

is considered constant across the sublayer, equation (42) can be integrated directly by use of an integrating factor. When the boundary conditions at the surface are employed, there results

$$i_1 - i_{1_w} + \frac{u^2}{2} = u_\infty^2 \left\{ \frac{\tilde{u}\left[F\tilde{u} + (c_f/2)\right]}{F} - \frac{\left[F\tilde{u} + (c_f/2)\right]^2}{(2 - Pr^*)F^2} + \frac{(c_f/2)^{2-Pr^*}}{(2 - Pr^*)F^2}\left(F\tilde{u} + \frac{c_f}{2}\right)^{Pr^*} \right\} + \frac{q_{c_w}}{\rho_\infty u_\infty F} \left\{ 1 - \left(\frac{c_f}{2}\right)^{-Pr^*}\left[F\tilde{u} + \left(\frac{c_f}{2}\right)\right]^{Pr^*} \right\} = \Gamma \tag{44}$$

To express equation (44) in terms of temperature, it is convenient to let $c_{p_1} = \text{const}$. At the sublayer side of the interface, then,

$$T_{a-} = \frac{\Gamma_a - (\tilde{u}_a^2/2)u_\infty^2}{c_{p_1}} + T_w \tag{45}$$

It is now necessary to determine the temperature on the turbulent side of the interface, T_{a+}, which will be matched to T_{a-} of equation (45). By integrating equation (28), there results

$$\rho_w v_w\left(i + \frac{u^2}{2}\right) = \epsilon_\lambda \frac{dT}{dy} + \rho\epsilon_d \frac{d\omega}{dy}(i_1 - i_2) + u\epsilon_v \frac{du}{dy} + C \tag{46}$$

Continuity at the interface of heat transfer due to diffusion and conduction, of shear, and of enthalpy and velocity requires the constant of integration of this equation to be the same as that for equation (40), namely, equation (41). To simplify the equation, di/dy is evaluated as

$$\frac{di}{dy} = \left.\frac{\partial i}{\partial T}\right|_\omega \frac{dT}{dy} + \left.\frac{\partial i}{\partial \omega}\right|_T \frac{d\omega}{dy} \tag{47}$$

By means of the definition of i, $i = i_1\omega + i_2(1 - \omega)$, it can be shown readily that when the turbulent Prandtl and Schmidt numbers are equal

$$\frac{\epsilon_v c_p}{\epsilon_\lambda} = \frac{\epsilon_v}{\rho\epsilon_d} \tag{48}$$

that substitution of equations (41), (47), and (48) into (46) results in

$$\rho_w v_w\left(i - i_{1_w} + \frac{u^2}{2}\right) - q_{c_w} = \frac{\epsilon_\lambda}{c_p}\frac{di}{dy} + u\epsilon_v \frac{du}{dy} \tag{49}$$

The independent variable is changed from y to u by dividing through by equation (34); thus

$$\frac{\rho_w v_w\left[i - i_{1_w} + (u^2/2)\right] - q_{c_w}}{\rho_w v_w u + \tau_w} = \frac{di}{du} + u \tag{50}$$

when, for simplicity, the turbulent Prandtl or Schmidt number is set equal to unity. When equation (50) is integrated with c_{p_2} set constant and the boundary conditions (16) are applied, there results

$$\frac{F + (c_f/2)}{F\tilde{u}_a + (c_f/2)} = \frac{F\left[c_{p_2}T_\infty - c_{p_1}T_w + (u_\infty^2/2)\right] - (q_{c_w}/\rho_\infty u_\infty)}{F\left[\omega_a c_{p_1}T_{a+} + (1 - \omega_a)c_{p_2}T_{a+} - c_{p_1}T_w + (u_a^2/2)\right] - (q_{c_w}/\rho_\infty u_\infty)} \tag{51}$$

When equation (51) is solved for T_{a+} and equated to the right member of equation (45), there results, after some manipulation,

$$\frac{q_{c_w}}{\rho_\infty u_\infty F} = \frac{c_{p_2}(T_w - T_\infty) - \sigma(u_\infty^2/2)}{\dfrac{F + (c_f/2)}{F\tilde{u}_a + (c_f/2)} - 1 - \dfrac{c_{p_a}}{c_{p_1}}\left\{\dfrac{F + (c_f/2)}{F\tilde{u}_a + (c_f/2)} - \dfrac{\left[F\tilde{u}_a + (c_f/2)\right]^{Pr^*-1}\left[F + (c_f/2)\right]}{(c_f/2)^{Pr^*}}\right\}} \tag{52}$$

where

$$F = \frac{\rho_w v_w}{\rho_\infty u_\infty}$$

and

$$\sigma = \left[1 - \tilde{u}_a^2 \frac{F + (c_f/2)}{F\tilde{u}_a + (c_f/2)}\right] - \frac{c_{p_a}}{c_{p_1}}\left\{\frac{2\tilde{u}_a\left[F + (c_f/2)\right]}{F} - \frac{2\left[F\tilde{u}_a + (c_f/2)\right]\left[F + (c_f/2)\right]}{(2 - Pr^*)F^2} + \frac{2(c_f/2)^{2-Pr^*}\left[F\tilde{u}_a + (c_f/2)\right]^{Pr^*-1}\left[F + (c_f/2)\right]}{(2 - Pr^*)F^2} - \tilde{u}_a^2 \frac{F + (c_f/2)}{F\tilde{u}_a + (c_f/2)}\right\} \tag{53}$$

If we let

$$q_{c_w} = h\left(T_w - T_\infty - \sigma \frac{u_\infty^2}{2c_{p_2}}\right) \tag{54}$$

and noting that $c_{p_2} = c_{p_\infty}$, then

$$\frac{St}{c_f/2} = \frac{F/(c_f/2)}{\dfrac{F(1 - \tilde{u}_a)}{F\tilde{u}_a + (c_f/2)} + \dfrac{c_{p_a}}{c_{p_1}}\left[\dfrac{F + (c_f/2)}{F\tilde{u}_a + (c_f/2)}\right]\left\{\dfrac{\left[F\tilde{u}_a + (c_f/2)\right]^{Pr^*}}{(c_f/2)^{Pr^*}} - 1\right\}} \tag{55}$$

Equation (55) represents the modified Reynolds analogy between heat transfer and skin friction when turbulent Prandtl and Schmidt numbers are unity. The term σ, defined in equation (53), is seen from equation (54) to be a temperature recovery factor.

Effect of Light-Gas Injection on Skin Friction of a Near Isothermal, Turbulent Boundary Layer

In order to evaluate the skin friction exerted by a turbulent boundary layer composed of a mixture of a light gas and air, the light

gas being transpired at the surface, it is necessary first to integrate the momentum equations (29) and (34) across the boundary layer. Because these equations contain the viscosity and density of the mixture (through μ and ϵ_v), integration of these equations in general must consider both the concentration and temperature variation across the boundary layer. In the preceding section it was shown that the local concentration and temperature could be related to the local velocity; therefore, it is possible to relate the local viscosity and density to the local velocity. Thus, integration of (29) results in the following equation written in a dimensionless form

$$R_y = \frac{\rho_\infty u_\infty y}{\mu_\infty} = \int_0^{\tilde{u}} \frac{(\mu/\mu_\infty)d\tilde{u}}{F\tilde{u} + (c_f/2)} \tag{56}$$

Before equation (34) can be integrated, it is necessary to express the eddy viscosity, ϵ_v, in terms of a mixing length. The usual expression obtained by employing the Prandtl mixing length concept is

$$\epsilon_v = \rho K^2 y^2 \frac{du}{dy} \tag{57}$$

Employing equation (57) with equation (34) yields

$$\rho_w v_w u + \tau_w = \rho K^2 y^2 \left(\frac{du}{dy}\right)^2 \tag{58}$$

When the root of both sides of equation (58) is taken, K is assumed a constant, and the resulting equation integrated from u_a to u, there is obtained in dimensionless form

$$R_y = R_{y_a} \exp\left[K \int_{\tilde{u}_a}^{\tilde{u}} \frac{(\rho/\rho_\infty)^{1/2} d\tilde{u}}{\sqrt{(c_f/2) + F\tilde{u}}}\right] \tag{59}$$

For the present, let it be considered that the boundary layer is nearly isothermal so that in integrating equations (56) and (59) it is not necessary to account for temperature variations. The viscosity and density thus become functions only of the concentration.

In the previous sections, the fluid properties within the sublayer, such as Schmidt number, have been treated as constants to simplify the integrations. The thought behind this simplification is that average values of the fluid properties in the sublayer should suffice for the calculations of the concentration, momentum, and energy in the sublayer. When this idea is carried over to the integration of equation (56), μ/μ_∞ is replaced by $(\mu/\mu_\infty)_{av}$, and there results

$$R_y = \left(\frac{\mu}{\mu_\infty}\right)_{av} \frac{1}{F} \ln \frac{F\tilde{u} + (c_f/2)}{c_f/2} \tag{60}$$

or

$$R_{y_a} = \left(\frac{\mu}{\mu_\infty}\right)_{av} \frac{1}{F} \ln \frac{F\tilde{u}_a + (c_f/2)}{c_f/2} \tag{61}$$

when R_y is evaluated at $\tilde{u}_a$, the interface.

In order to integrate equation (59) in the turbulent portion of the boundary layer, it is convenient to employ the density variation

$$\frac{\rho}{\rho_\infty} = \frac{1}{\left[(M_2/M_1) - 1\right]\omega + 1} \tag{62}$$

This equation applies to an isothermal boundary layer on a flat plate and has been obtained from Dalton's law for partial pressures and the perfect gas law. Equation (62) must be expressed in terms of the local velocity to facilitate integrating equation (59). From equation (37), when $Sc' = 1$,

$$1 - \omega = \frac{F\tilde{u} + (c_f/2)}{F + (c_f/2)} \tag{63}$$

Combining equations (62) and (63) results in

$$\frac{\rho}{\rho_\infty} = \frac{1}{m - n\tilde{u}} \tag{64}$$

where

$$\left.\begin{aligned} m &= \frac{M_2}{M_1} - \left(\frac{M_2}{M_1} - 1\right) \frac{c_f/2}{F + (c_f/2)} \\ n &= \left(\frac{M_2}{M_1} - 1\right) \frac{F}{F + (c_f/2)} \end{aligned}\right\} \tag{65}$$

Use of equation (64) permits integration of the argument of the exponent in equation (59) to yield for $n > 0$ (light-gas injection)

$$\ln \frac{R_y}{R_{y_a}} = \frac{-K}{\sqrt{Fn}} \left[\sin^{-1} \frac{-2Fn\tilde{u} - n(c_f/2) + mF}{n(c_f/2) + mF} - \sin^{-1} \frac{-2Fn\tilde{u}_a - n(c_f/2) + mF}{n(c_f/2) + mF} \right] \tag{66a}$$

and for $n < 0$ (heavy-gas injection)

$$\ln \frac{R_y}{R_{y_a}} = \frac{2K}{\sqrt{-Fn}} \left[\tanh^{-1} \sqrt{\frac{-n\left[F\tilde{u} + (c_f/2)\right]}{F(m - n\tilde{u})}} - \tanh^{-1} \sqrt{\frac{-n\left[F\tilde{u}_a + (c_f/2)\right]}{F(m - n\tilde{u}_a)}} \right] \tag{66b}$$

Equations (60) and (66) represent the expressions for velocity distribution in the boundary layer.

These velocity distributions will be used to obtain skin-friction expressions. Note that only the turbulent velocity distribution is used in the integration for the momentum thickness. From reference 3, the skin-friction integral equation under conditions of surface injection is

$$\frac{c_f}{2} + F = \frac{d}{dx} \int_0^1 \left(\frac{\rho}{\rho_\infty}\right) \tilde{u}(1 - \tilde{u}) \frac{dy}{d\tilde{u}} \, d\tilde{u} = \frac{d\theta}{dx} \tag{67}$$

where the integral term represents the momentum thickness, θ.

From equation (59) it can be deduced that

$$\frac{dy}{d\tilde{u}} = y_a \frac{K(\rho/\rho_\infty)^{1/2}}{\sqrt{(c_f/2) + F\tilde{u}}} \exp\left[K \int_{\tilde{u}_a}^{\tilde{u}} \frac{(\rho/\rho_\infty)^{1/2} \, d\tilde{u}}{\sqrt{(c_f/2) + F\tilde{u}}} \right] \tag{68}$$

If the exponential term is represented by the symbol, g, the right member of (68) is $y_a(dg/d\tilde{u})$. Substitution of equation (68) into the integral representing θ results in

$$\theta = y_a \int_0^1 \frac{\rho}{\rho_\infty} \tilde{u}(1 - \tilde{u}) \frac{dg}{d\tilde{u}} \, d\tilde{u} \tag{69}$$

When use is made of equation (64) and the independent variable is changed to g, equation (69) becomes

$$\theta = y_a \int_{g(0)}^{g(1)} \frac{\tilde{u}(1 - \tilde{u})}{m - n\tilde{u}} \, dg \tag{70}$$

When equation (70) is integrated by parts, there results

$$\theta = y_a \left[\frac{\tilde{u}(1 - \tilde{u})}{m - n\tilde{u}} \, g \Big|_0^1 - \int_0^1 g \, \frac{(1 - 2\tilde{u})(m - n\tilde{u}) + n\tilde{u}(1 - \tilde{u})}{(m - n\tilde{u})^2} \, d\tilde{u} \right] \tag{71}$$

Since $g(0)$ and $g(1)$ are finite, the first term vanishes because of the boundary conditions $\tilde{u} = 0$ at the wall and $\tilde{u} = 1$ at the outer edge of the boundary layer. From (68) and the definition of g

$$g\,d\tilde{u} = \frac{\sqrt{(c_f/2) + F\tilde{u}}}{K(\rho/\rho_\infty)^{1/2}}\,dg = \frac{\sqrt{m - n\tilde{u}}\,\sqrt{(c_f/2) + F\tilde{u}}}{K}\,dg \tag{72}$$

Using (72), equation (71) becomes

$$\theta = -y_a \int_{g(o)}^{g(1)} \frac{\sqrt{(c_f/2) + F\tilde{u}}\,(m - 2m\tilde{u} + n\tilde{u}^2)dg}{K(m - n\tilde{u})^{3/2}} \tag{73}$$

Again, integrating equation (73) by parts (noting that $g(1) \gg g(0)$ and for $\sqrt{(c_f/2) + F} \gg (c_f/2) + F$) and retaining only the largest terms, yields

$$R_\theta = R y_a \frac{g(1)}{K}\sqrt{\frac{c_f}{2} + F} \tag{74}$$

Equation (74) represents the relationship between the local skin-friction coefficient and the local Reynolds number based on momentum thickness.

To obtain the relationship between the local skin-friction coefficient and the Reynolds number based on length of run, it is necessary to employ equation (67) in the form

$$\frac{c_f}{2} + F = \frac{d\theta}{dx} = \frac{dR_\theta}{dR_x} \tag{75}$$

On integrating equation (75) there results

$$R_x = \int_o^{R_\theta} \frac{dR_\theta}{(c_f/2) + F} \tag{76}$$

if the start of the boundary layer is at $R_x = 0$. By the use of equation (74) equation (76) can be transformed to

$$R_x = \int_{c_f=\infty}^{c_f/2} \frac{d\left\{R y_a \left[g(1)/K\right]\sqrt{(c_f/2) + F}\right\}}{(c_f/2) + F} \tag{77}$$

With the use of the relations for $R y_a$, $g(1)$, and $\dfrac{dg(1)}{d\left[(c_f/2) + F\right]}$, repeated integration of equation (77) by parts results in

$$R_x = \frac{R_{y_a} g(1)}{K\sqrt{(c_f/2) + F}}\Bigg|_{\infty}^{c_f/2} + \begin{matrix}\text{smaller}\\ \text{additional}\\ \text{terms}\end{matrix} \tag{78}$$

When the boundary values are imposed, there results

$$R_x = \frac{R_{y_a} g(1)}{K\sqrt{(c_f/2) + F}} \tag{79}$$

Equation (79) represents the relationship between the local skin-friction coefficient and the local Reynolds number based on length of run. In both (74) and (79), g(1) is defined for light-gas injection ($n > 0$)

$$g(1) = \exp\left\{-\frac{K}{\sqrt{Fn}}\left[\sin^{-1}\frac{-2Fn - n(c_f/2) + mF}{n(c_f/2) + mF} - \sin^{-1}\frac{-2Fn\tilde{u}_a - n(c_f/2) + mF}{n(c_f/2) + mF}\right]\right\} \tag{80}$$

and for heavy-gas injection ($n < 0$)

$$g(1) = \exp\left(\frac{2K}{\sqrt{-Fn}}\left\{\tanh^{-1}\sqrt{\frac{-n\left[F + (c_f/2)\right]}{F}} - \tanh^{-1}\sqrt{\frac{-n\left[F\tilde{u}_a + (c_f/2)\right]}{F(m - n\tilde{u}_a)}}\right\}\right)$$

RESULTS AND DISCUSSION

Before the end results of the analysis could be evaluated numerically, it was necessary to determine for the gas mixtures considered the molecular transport properties, viscosity, thermal conductivity, and diffusion coefficient, which can be combined to yield Schmidt and Prandtl numbers. The viscosity was determined by the method of Wilke (ref. 12); the thermal conductivity, by the method of Lindsay and Bromley (ref. 13); and the diffusion coefficient, by the method of Hirschfelder, Curtiss, and Bird (ref. 11). These methods have been recently summarized and compared with other available methods by Carlson and Schneider (ref. 14). It can be concluded from the latter paper that the methods used in this report are in keeping with the present knowledge of the molecular transport mechanism in binary gaseous mixtures.

The results of these calculations are shown in figures 1 through 5 for both helium-air and hydrogen-air mixtures at a temperature of 500° R. Figure 1 shows the variation of the viscosity of the mixture with the mass fraction of the light gas. It is observed that the viscosities of the mixtures vary continuously as the mixture concentration is changed; however,

it is interesting to note that the viscosity of the helium-air mixture can exceed the viscosity of the pure individual constituents. The corresponding thermal conductivity of the gas mixtures is shown in figure 2. The results of these figures are combined with the specific heats of the mixtures, $c_p = c_{p_1}\omega + c_{p_2}(1 - \omega)$, to form the mixture Prandtl numbers shown in figure 3. It should be noted that small concentrations of the light gas, $\omega \approx 0.1$, markedly reduce the Prandtl number of the mixture from the value of either of the pure constituents in both mixtures. Values as low as 0.42 and 0.46 result for the hydrogen-air and helium-air mixtures, respectively. The Prandtl number, Pr^*, defined by equation (43), in which the specific heat used is that of the light gas, rather than that for the mixture, is shown plotted in figure 4. It is seen that Pr^* varies considerably with variations of the mass fraction of the light gas, especially at the lower values of ω. The importance of this large variation of Pr^* is discussed later in conjunction with the discussion of the heat-transfer results. The Schmidt numbers for the gas mixtures are shown in figure 5; the diffusion coefficient used for these calculations was determined by means of the equations of reference 11 for a temperature of 500° R and a pressure of one atmosphere. It is seen that the Schmidt number varies considerably with the mass fraction of the light gas, the increase being largely due to the decrease in density of the mixture.

It is recalled that in the Analysis, integrations across the laminar sublayer were performed considering the Schmidt number, Sc, the Prandtl number, Pr^*, and the viscosity ratio, μ/μ_∞, constant and equal to the average value in the sublayer. This was done to simplify the integrations and was thought to be justified by the thinness of the sublayer so that only small changes in the transport parameters were expected. To check this, curves such as shown in figure 6 were evaluated from the numerical results. In this figure there is shown the surface and interface concentration of the light gases as a function of the injection rate parameter, ζ, which is equal to the local dimensionless injection rate, F, divided by the local skin-friction coefficient, $c_f/2$. These curves apply to a position where the length Reynolds number is 10 million. It is seen that the concentrations of the light gases change about 20 percent through the sublayer over most of the ζ range shown. From figures 4 and 5, it can be seen that a 20-percent change in concentration, depending on the value of ω, can produce large changes in Pr^* and Sc. It became necessary to investigate what effects these changes could produce in the end results. In the determination of ω_w from equation (32), where ω_a is obtained from equation (37), the procedure followed was to estimate the Schmidt number, calculate ω_w and then determine a new Schmidt number as

$$Sc = Sc\left(\frac{\omega_a + \omega_w}{2}\right)$$

This Schmidt number was then used in equation (32) to re-evaluate ω_w. The iteration procedure converged rapidly and required only two steps.

A variable Schmidt number which was linear with concentration was used to integrate the equations leading to equation (32). The latter results were more complicated algebraically and were not significantly different from those of the simpler equation (32). The additional complications of permitting the Schmidt number to vary, therefore, were not warranted.

Once the concentration variations across the sublayer were evaluated, it was possible to determine the degree of approximation involved in using average Pr^* and μ/μ_∞ across the sublayer. It was found that using the Pr^* corresponding to the extreme values of ω_a and ω_w in equation (55) produced only about a 3-percent variation in Stanton number, with the answers based on $Pr^*\left(\frac{\omega_a + \omega_w}{2}\right)$ lying roughly halfway between the extremes. This would indicate that the effects of the variations in Pr^* were not significant. Also, substituting the extreme value of viscosity associated with ω_a and ω_w resulted in, at most, a variation of 2 percent in the skin-friction coefficient when plotted against length Reynolds number; again this is not deemed significant. It can be concluded that the simplified mathematical steps of the analysis do not introduce large errors and are adequate for an exploratory type of analysis such as this.

Besides providing information for assessing the accuracy of the calculations, the curves in figure 6 provide interesting information from the physical viewpoint. The curves of ω_w show how the concentration of the light gas at the surface increases with increased injection. Only at the highest injection rates shown does ω_w approach unity or the all light-gas condition. At the low injection rates, $\zeta < 1$, the gas at the surface is composed mostly of air.

Numerical evaluation of equation (79) employing equations (61) and (80), with $K = 0.392$ and $\tilde{u}_a = 13.1\sqrt{c_f/2}$ (ref. 3), results in the values of skin-friction coefficient shown in figures 7(a) and 7(b) for helium and hydrogen injection into an isothermal boundary layer. The parameter of the curves is the term ζ and was chosen because the condition of a fixed ζ results in nearly a constant surface temperature with transpiration cooling. The $\zeta = 0$ curve is from reference 3. In general, it is noted from either figure that increased injection, larger ζ, causes the skin friction to diminish. This lowering occurs quite uniformly over the entire range of Reynolds numbers shown.

The effect of injection in reducing the skin friction is shown more clearly in figures 8(a) and 8(b). Here, the ordinate represents the ratio of the skin-friction coefficient to its corresponding value at zero injection. The abscissa is the ratio of the local dimensionless injection rate divided by the local skin-friction coefficient corresponding to zero injection. From the numerical results of reference 3 it can be shown that these dimensionless groups are convenient coordinates to show the effect on skin friction due to <u>air</u> injection in nonisothermal boundary layers because the effects of Mach number, wall to free-stream temperature, and Reynolds number are largely diminished by use of these

coordinates. Thus, in an analogous manner, it is considered that the isothermal boundary-layer results shown in these figures may be indicative of what occurs more generally. Again, the large reductions of skin friction by the injection of either of the two gases are evident for each of the Reynolds numbers shown.

A comparison of the relative effectiveness in reducing skin friction by injection of helium, hydrogen, and air (ref. 3) is shown in figure 9. The value $R_x = 10^7$ is picked for this comparison. It is apparent that the light gases are much more effective than air in reducing skin friction. For instance, a 50-percent reduction in skin friction would require mass-flow rates for hydrogen, helium, and air in the proportion of 0.21 : 0.394 : 1.0; or looking at the results in a different way, a mass-flow rate of $F/(c_f/2)_o = 0.80$ would cause skin-friction reductions of 89, 62, and 29.5 percent for hydrogen, helium, and air, respectively.

If the restriction that the boundary layer is isothermal is relaxed sufficiently to permit some heat transfer without altering to any significant extent the properties of the gas, it is possible to determine the effect of injection on the heat transfer by means of the preceding calculations of the skin friction. These heat-transfer results can be expressed in terms of Stanton number and temperature recovery factor.

The effect of surface injection of light gases on Stanton number is shown in figures 10(a) and 10(b). Here the ratio of Stanton number to its value for zero injection is plotted for three Reynolds numbers against the dimensionless injection rate, F, divided by the Stanton number corresponding to zero injection, St_o. This coordinate system, as in the coordinate system used for skin friction, has been found convenient for air injection to diminish the effects of Mach number, Reynolds number, and ratio of wall to free-stream temperature. It is believed that this coordinate system may tend to generalize the present results to conditions that differ from a nearly isothermal boundary layer.

It may be seen from figures 10(a) and 10(b) that increasing the injection rate from a zero value at first increases the Stanton number slightly. At higher injection rates the Stanton number is reduced in a manner similar to that of the skin friction. The slight increase in the Stanton number for the low injection rate can be explained by examining equation (55). The denominator of the right member is seen to be composed of the sum of two terms. The first term, called α and given by

$$\alpha = \frac{F(1 - \tilde{u}_a)}{F\tilde{u}_a + (c_f/2)} = \frac{\zeta(1 - \tilde{u}_a)}{\zeta\tilde{u}_a + 1} \tag{81}$$

can be considered to be proportional to the resistance to heat flow of the outer turbulent portion and, similarly, the second term β where

$$\beta = \frac{c_{p_a}}{c_{p_1}}\left[\frac{F + (c_f/2)}{F\tilde{u}_a + (c_f/2)}\right]\left\{\frac{\left[F\tilde{u}_a + (c_f/2)\right]^{Pr^*}}{(c_f/2)^{Pr^*}} - 1\right\} = \frac{c_{p_a}}{c_{p_1}}\left(\frac{\zeta + 1}{\zeta\tilde{u}_a + 1}\right)\left[(\zeta\tilde{u}_a + 1)^{Pr^*} - 1\right] \tag{82}$$

is proportional to the resistance to heat flow of the laminar sublayer. For instance, if $\tilde{u}_a = 0$, and there is no sublayer, β has the value zero and all the resistance to heat flow occurs in the outer turbulent portion. If $\tilde{u}_a = 1$, it is seen that the converse is true, that is, all the resistance to heat flow would be due to the laminar portion of the boundary layer because α is now zero. Now then, what happens at very low injection rates? When F, or ζ, is small, β can be rewritten by expanding the last bracketed term in a series, thus,

$$\beta = \frac{c_{p_a}}{c_{p_1}}\left(\frac{\zeta + 1}{\zeta\tilde{u}_a + 1}\right)\left[Pr^*\zeta\tilde{u}_a + \frac{Pr^*(Pr^* - 1)}{2}\zeta^2\tilde{u}_a^2 + \ldots\right] \tag{83}$$

or

$$\lim_{\zeta \to 0} \beta = \frac{c_{p_a}}{c_{p_1}} Pr^*\zeta\tilde{u}_a = Pr_{av}\frac{c_{p_a}}{c_{p_{av}}}\zeta\tilde{u}_a$$

It is seen that for small injection rates, the resistance of the sublayer to heat transfer is proportional to the Prandtl number, evaluated at the average concentration in the sublayer and to the ratio $c_{p_a}/c_{p_{av}}$. Note that for light gases $c_{p_a}/c_{p_{av}} < 1$ since $\omega_a < \omega_{av}$ and $c_{p_1} > c_{p_2}$. To illustrate the behavior of α and β numerically, an example is considered using equations (81) and (83). For hydrogen injection at $F/St_o = 0.046$ and $R_x = 10^6$, the average concentration of hydrogen, by weight, in the sublayer is found from a figure such as figure 6 to be about 3 percent. It is noted from figure 3 that this small concentration of hydrogen causes a decrease of 30 percent in the Prandtl number of the mixture in the sublayer. For these conditions, the term β is equal to 0.016. Now, if this drop in Prandtl number did not occur, that is, if the Prandtl number and the specific heat remained that of air, then the term β would be equal to 0.0242 and the resistance to heat flow in the sublayer would be increased. Since the value of α is 0.0277, the total resistance to heat flow through the whole boundary layer is 16 percent less for the binary mixture than for the case where the Prandtl number and specific heat were the values of air. This tendency to decrease the resistance to heat flow, or to increase the Stanton number, appears for the lower injection rates to be larger than the normal tendency of the injection process alone to reduce Stanton number. At the high injection rates, the effect of property changes to increase the Stanton number becomes smaller and the effect of the injection process alone becomes larger so as to predominate, and causes the decrease of Stanton number with injection shown in figure 10(b). A similar explanation applies for the case of helium.

A comparison of the relative reduction of heat transfer by injection of hydrogen, helium, and air into the turbulent boundary layer is shown in figure 11. The comparison is made for $R_x = 10^7$. It is evident that the light gases when injected into the boundary layer are more effective than air in reducing the heat transfer. To reduce the heat transfer to 50 percent of the zero injection value requires mass-flow rates of hydrogen, helium, and air in the proportion of 0.19 : 0.42 : 1.0. As another method of comparison, a mass-flow rate of F/St_o of 0.80 will cause heat-transfer reductions of 90, 60, and 27.5 percent for hydrogen, helium, and air, respectively. Included in figure 11 are the experimental data of Leadon and Scott, reference 15, for injection of helium and air into a turbulent boundary layer for $R_x = 4 \times 10^6$, at a Mach number 3.0, and a wall to free-stream temperature ratio of 3.30. The curve for air is obtained from reference 3 for Mach number zero and wall temperature equal to free-stream temperature, that is, a nearly isothermal boundary layer. The agreement between theory and experiment is good for air injection. If it is assumed that the present theoretical heat-transfer results for the helium injection are generalized by the coordinate system of figure 11 as they are for air, then it is seen that for helium injection the theory does not agree closely with experiment but certainly indicates the relative advantages of helium injection.

A comparison of the variation of recovery factor with injection of hydrogen, helium, and air is shown in figure 12 for $R_x = 10^7$. The zero injection value, σ_o, and the recovery-factor curve for air have been obtained from reference 3. The dip in the curves for the low injection rates for both hydrogen and helium as contrasted to air may be explained by the reduction of the Prandtl number within the sublayer of the boundary layer. Comparison with the experimental results of Leadon and Scott, reference 15, clearly shows that the theoretical curves do not indicate the trends of the experimental recovery factor with injection for either helium or air. The disagreement between theory and experiment, evident in this figure, emphasizes the need for improving the present theory before it can be applied with confidence to predict recovery factors.

CONCLUDING REMARKS

A mixing length theory in which it is assumed that both the turbulent Schmidt and Prandtl numbers are unity has been developed for the case of the injection of foreign gases into the air of a turbulent boundary layer. It has been found that:

1. From the viewpoint of reducing skin friction by injection, helium and hydrogen are generally 2.5 and 5.0 times as effective as air on a mass basis.

2. From the viewpoint of reducing Stanton number by injection, helium and hydrogen are generally 2.4 and 5.2 times as effective as air on a mass basis.

3. There are no major effects on temperature-recovery factor due to the injection of helium and hydrogen.

At present, no data exist for evaluating the results of item 1. For item 2, however, experimental results generally confirm the high effectiveness of the light gases in reducing the Stanton number, although there does not exist exact quantitative agreement between theory and experiment. For item 3, the theory does not even indicate the general trends of the experimental temperature-recovery factors.

Even though mixing length theory is known to be basically incorrect, many useful results have been obtained through its use. It has been shown in reference 16 in which a mixing length theory was used that taking account of variations in the shear distribution across the boundary layer and permitting deviations of the turbulent Prandtl number from unity have improved the representation of the Stanton number and particularly the temperature-recovery factor of a single-constituent gas. From this it is indicated that the present analysis should be extended to incorporate variations in shear across the boundary layer and deviations from unity of the turbulent Schmidt and Prandtl numbers.

Ames Aeronautical Laboratory
National Advisory Committee for Aeronautics
Moffett Field, Calif., Nov. 18, 1957

REFERENCES

1. Eckert, E. R. G., and Livingood, John N. B.: Comparison of Effectiveness of Convection-, Transpiration-, and Film-Cooling Methods With Air as Coolant. NACA Rep. 1182, 1954. (Supersedes NACA TN 3010)

2. Dorrance, William H., and Dore, Frank J.: The Effect of Mass Transfer on the Compressible Turbulent Boundary-Layer Skin Friction and Heat Transfer. Jour. Aero. Sci., vol. 21, no. 6, June 1954, pp. 404-410.

3. Rubesin, Morris W.: An Analytical Estimation of the Effect of Transpiration Cooling on the Heat-Transfer and Skin-Friction Characteristics of a Compressible, Turbulent Boundary Layer. NACA TN 3341, 1954.

4. Mickley, H. S., Ross, R. C., Squyers, A. L., and Stewart, W. E.: Heat, Mass, and Momentum Transfer for Flow Over a Flat Plate With Blowing or Suction. NACA TN 3208, 1954.

5. Brown, W. Byron, and Donoughe, Patrick L.: Tables of Exact Laminar-Boundary-Layer Solutions When the Wall is Porous and Fluid Properties are Variable. NACA TN 2479, 1951.

6. Low, George M.: The Compressible Laminar Boundary Layer With Fluid Injection. NACA TN 3404, 1955.

7. Eckert, E. R. G., and Schneider, P. J.: Diffusion Effects in Binary Isothermal Boundary Layer. Tech. Rep. 5, Inst. of Tech., Mech. Engr. Dept., Heat Transfer Lab., Univ. of Minnesota, Nov. 1955.

8. Eckert, E. R. G., Schneider, P. J., and Koehler, F.: Mass Transfer Cooling of a Laminar Air Boundary Layer by Injection of a Light-Weight Gas. Tech. Rep. 8, Inst. of Tech., Mech. Engr. Dept., Heat Transfer Lab., Univ. of Minnesota, Apr. 1956.

9. Townsend, A. A.: The Structure of the Turbulent Boundary Layer. Proc. Cambridge Phil. Soc., vol. 47, pt. 2, Apr. 1951, pp. 375-395.

10. Rubesin, Morris W., Maydew, Randall C., and Varga, Steven A.: An Analytical and Experimental Investigation of the Skin Friction of the Turbulent Boundary Layer on a Flat Plate at Supersonic Speeds. NACA TN 2305, 1951.

11. Hirschfelder, Joseph O., Curtiss, Charles F., and Bird, R. Byron: Molecular Theory of Gases and Liquids. John Wiley & Sons, New York, 1954.

12. Wilke, C. R.: A Viscosity Equation for Gas Mixtures. Jour. Chem. Phys., vol. 18, no. 4, Apr. 1950, pp. 517-519.

13. Lindsay, Alexander L., and Bromley, LeRoy A.: Thermal Conductivity of Gas Mixtures. UCRL-461, University of California Radiation Lab., Sept. 1949.

14. Carlson, W. O., and Schneider, P. J.: Transport Properties for Binary Gas Mixtures. Tech. Rep. 7, Inst. of Tech., Mech. Engr. Dept., Heat Transfer Lab., Univ. of Minnesota, Jan. 1956.

15. Leadon, B. M., and Scott, C. J.: Measurement of Recovery Factors and Heat Transfer Coefficients With Transpiration Cooling in a Turbulent Boundary Layer at $M = 3.0$ Using Air and Helium as Coolants. Res. Rep. 126, Inst. of Tech., Mech. Engr. Dept., Heat Transfer Lab., Dept. of Aero. Engr., Rosemount Aero. Lab., Univ. of Minnesota, Feb. 1956.

16. Van Driest, E. R.: The Turbulent Boundary Layer With Variable Prandtl Number. Rep. AL-1914, North American Aviation, Inc., Apr. 1954.

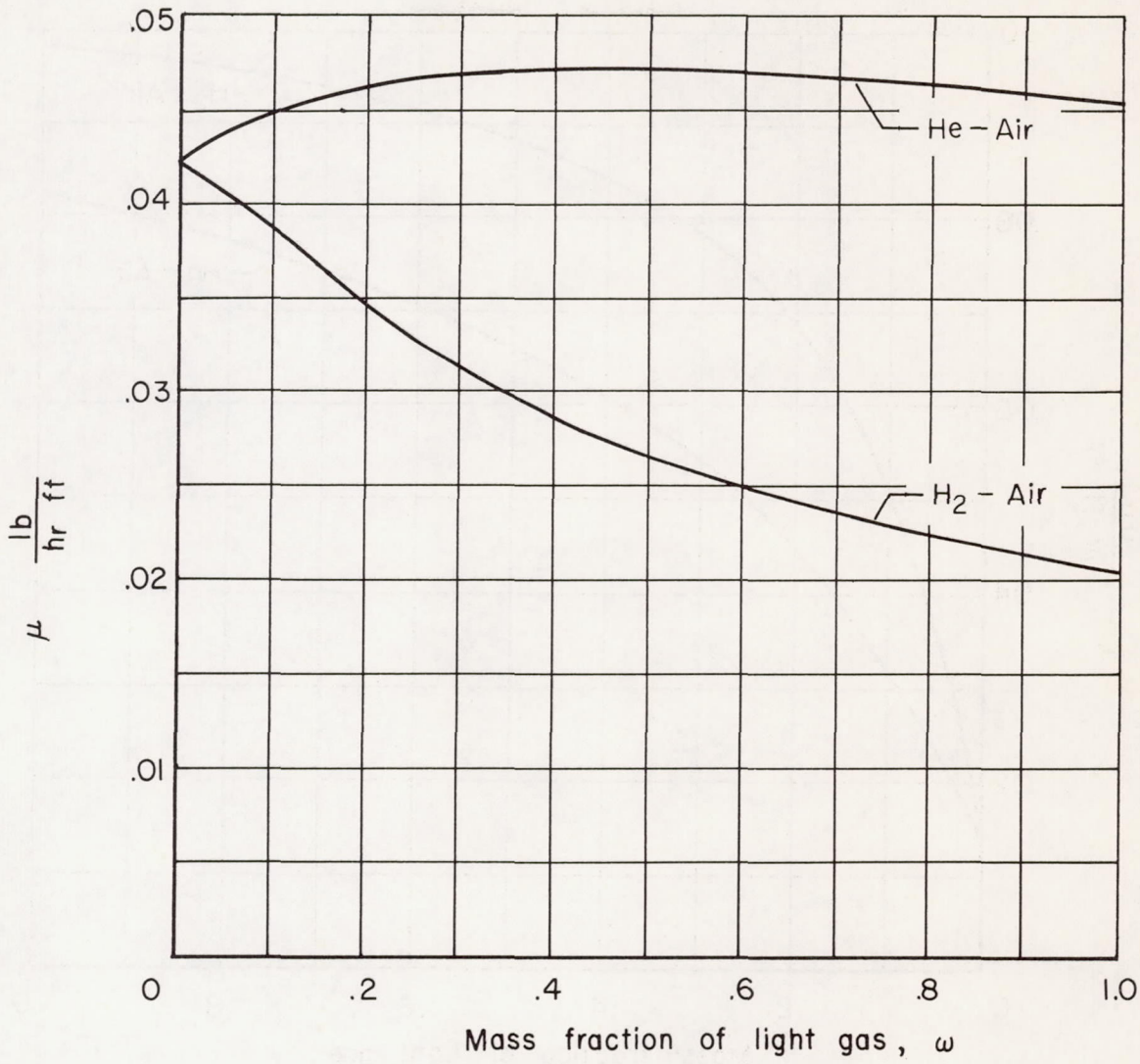

Figure 1.- Viscosity of binary gas mixtures; T = 500° R; method of Wilke, reference 12.

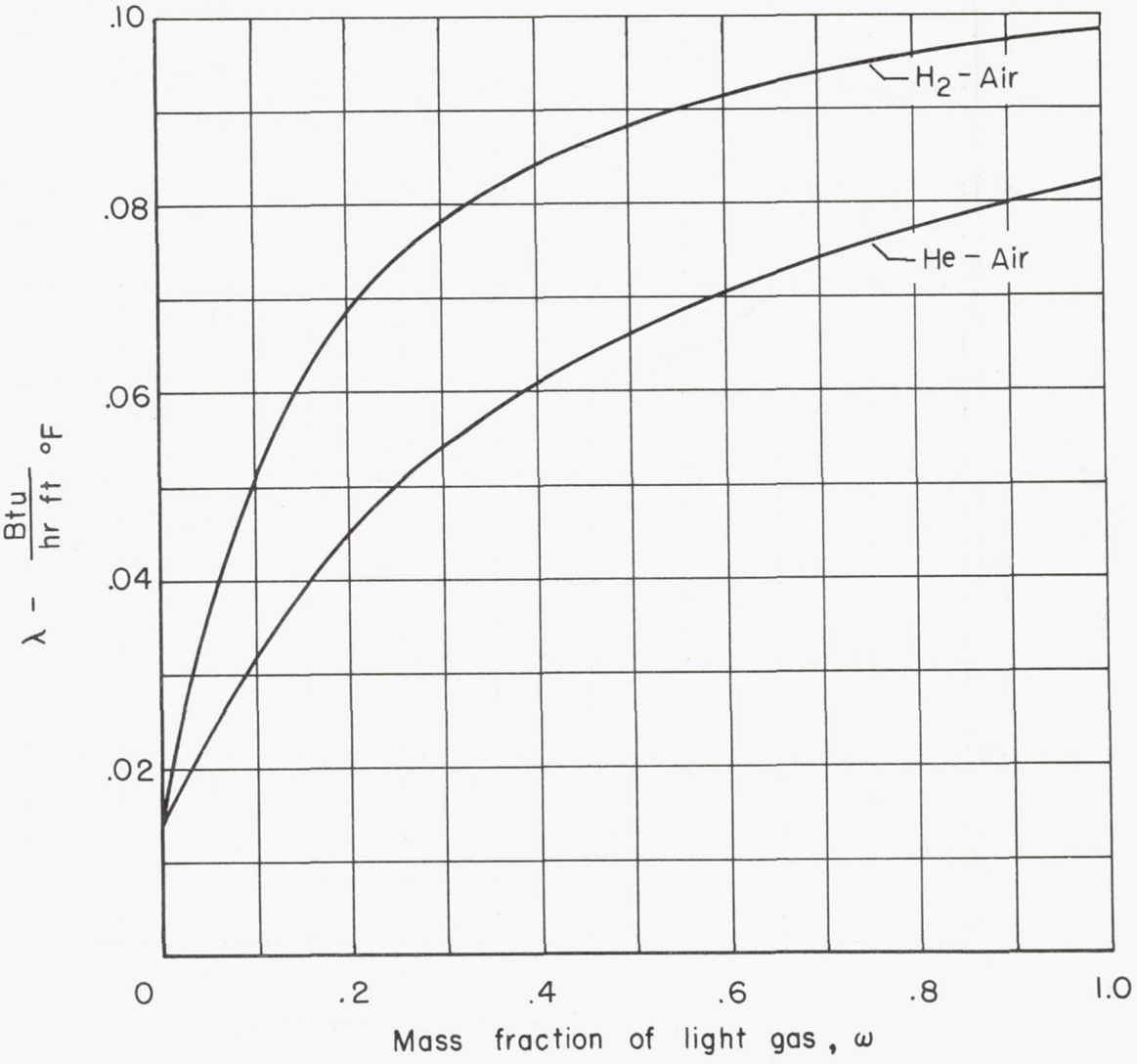

Figure 2.- Thermal conductivity of binary gas mixtures; T = 500° R; method of Lindsay and Bromley, reference 13.

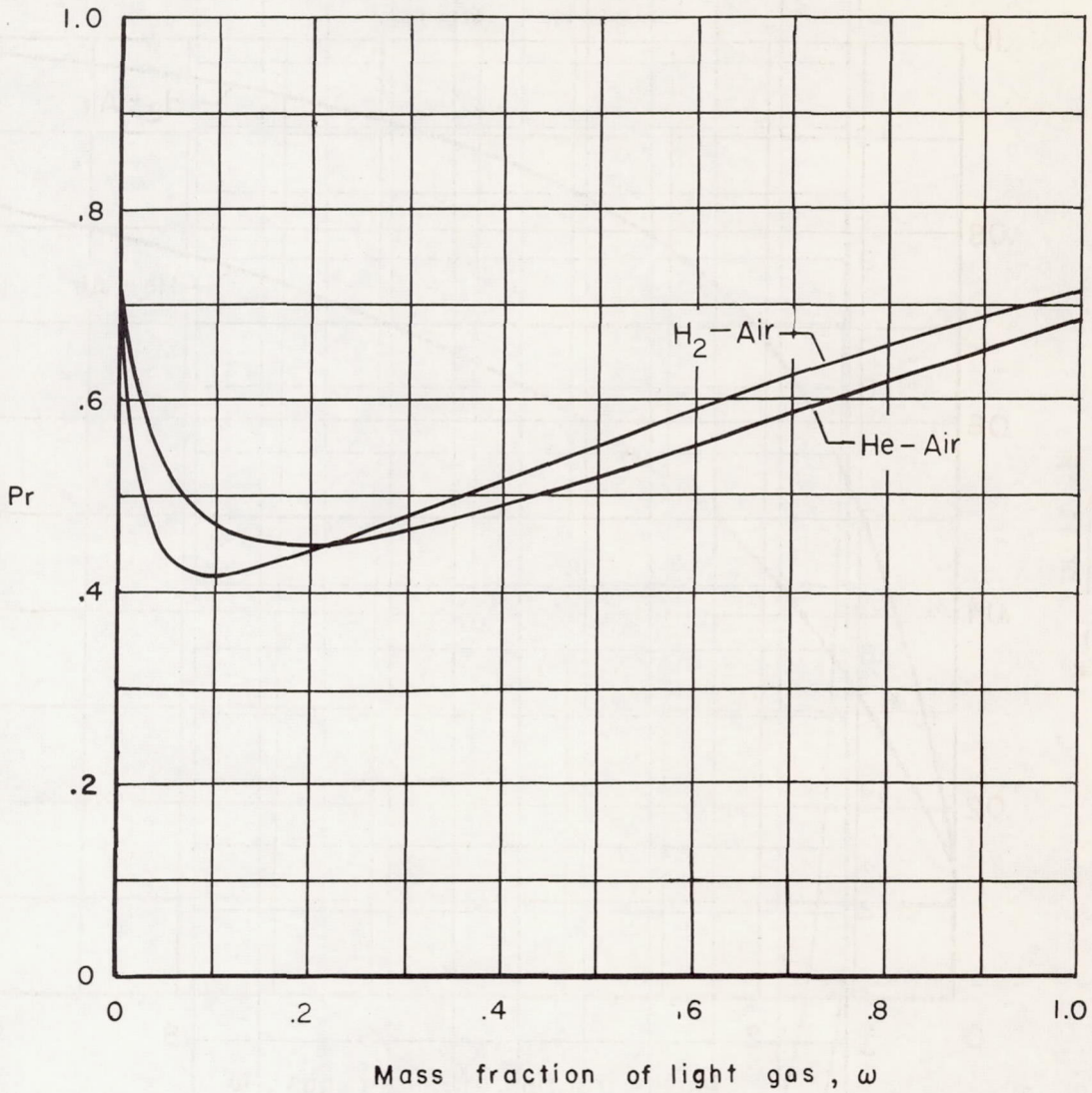

Figure 3.- Prandtl number of binary gas mixtures; T = 500° R.

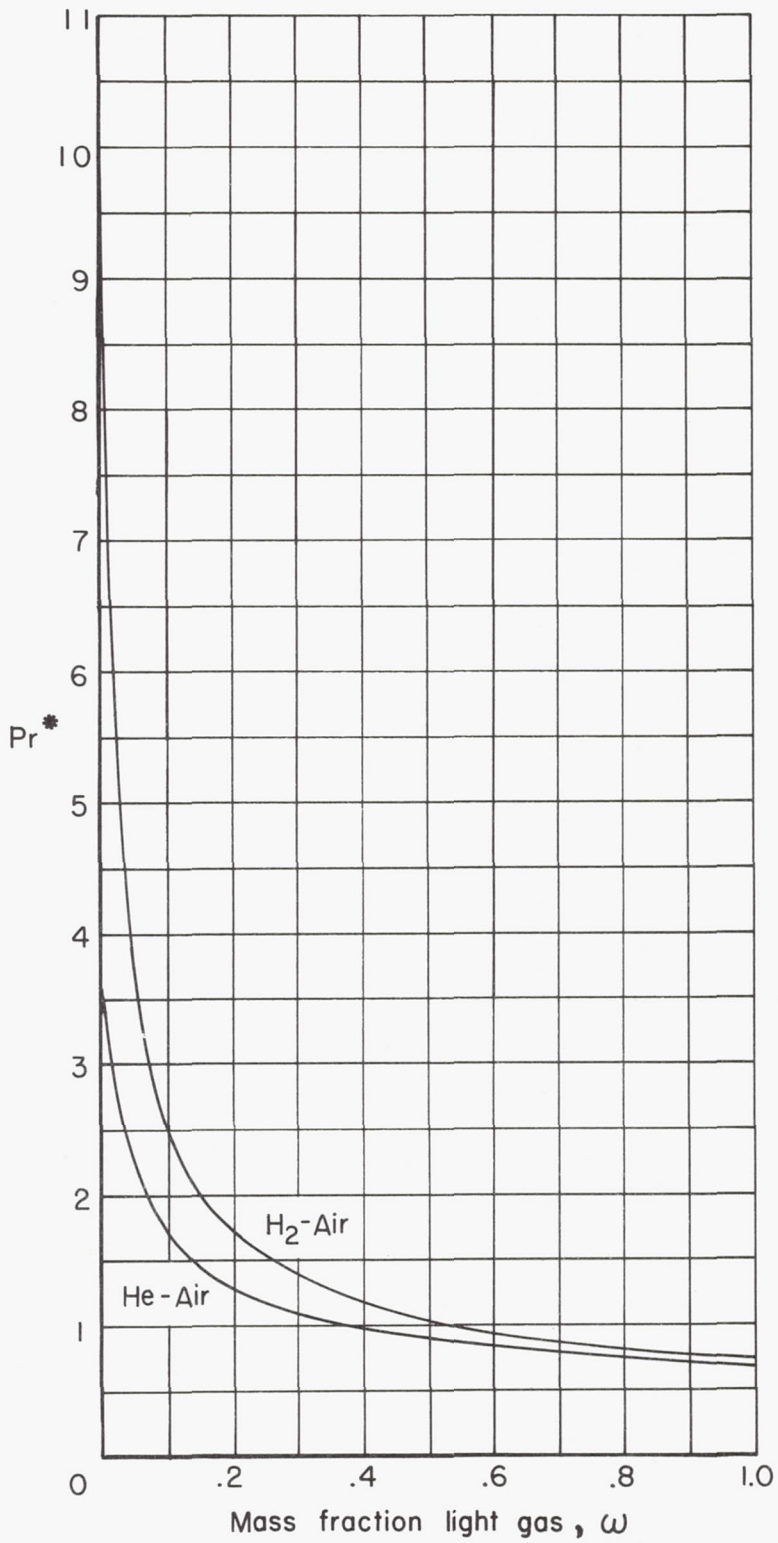

Figure 4.- Variation of Pr^* with light-gas mass fraction; T = 500° R.

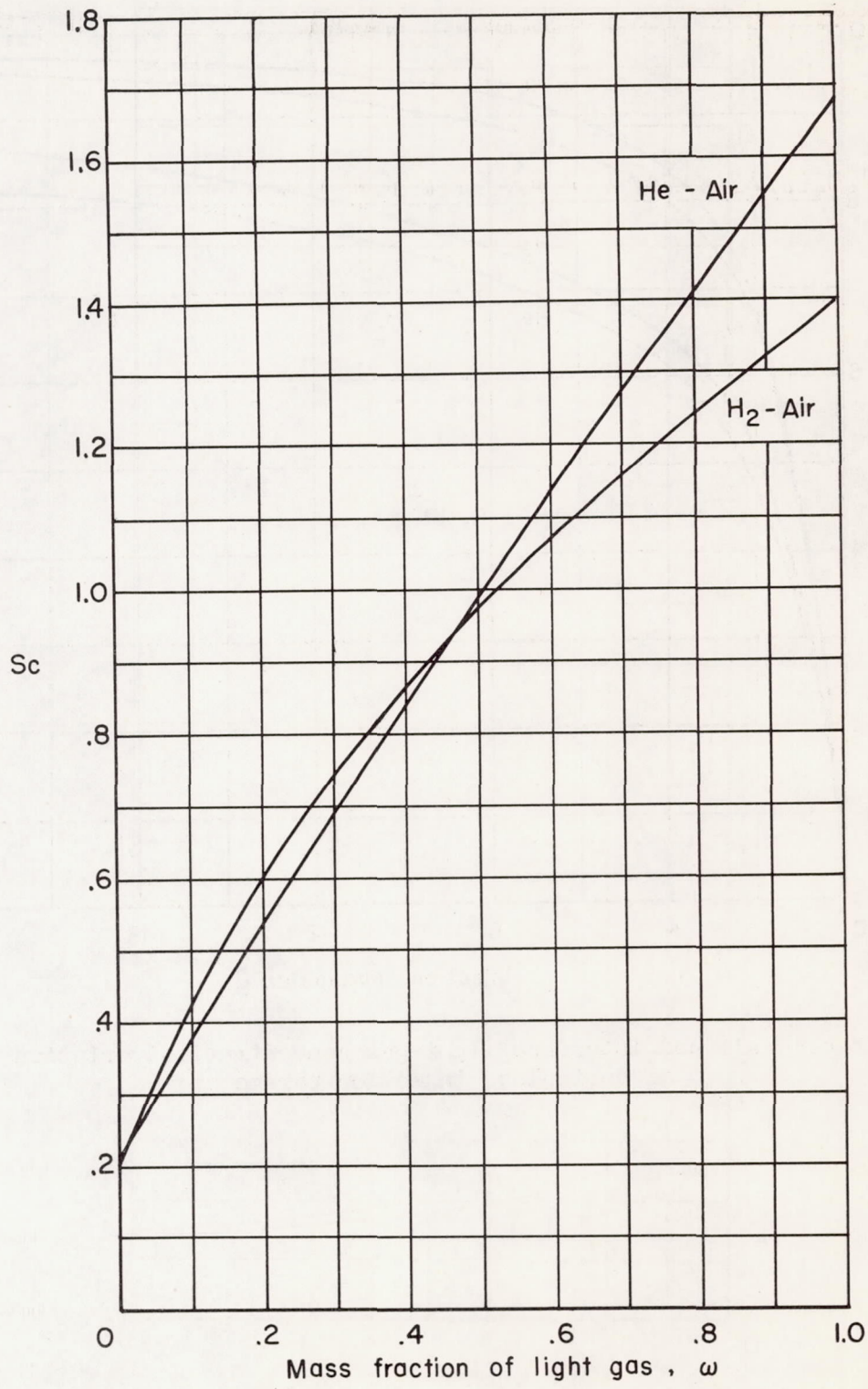

Figure 5.- Schmidt number of binary gas mixtures; T = 500° R.

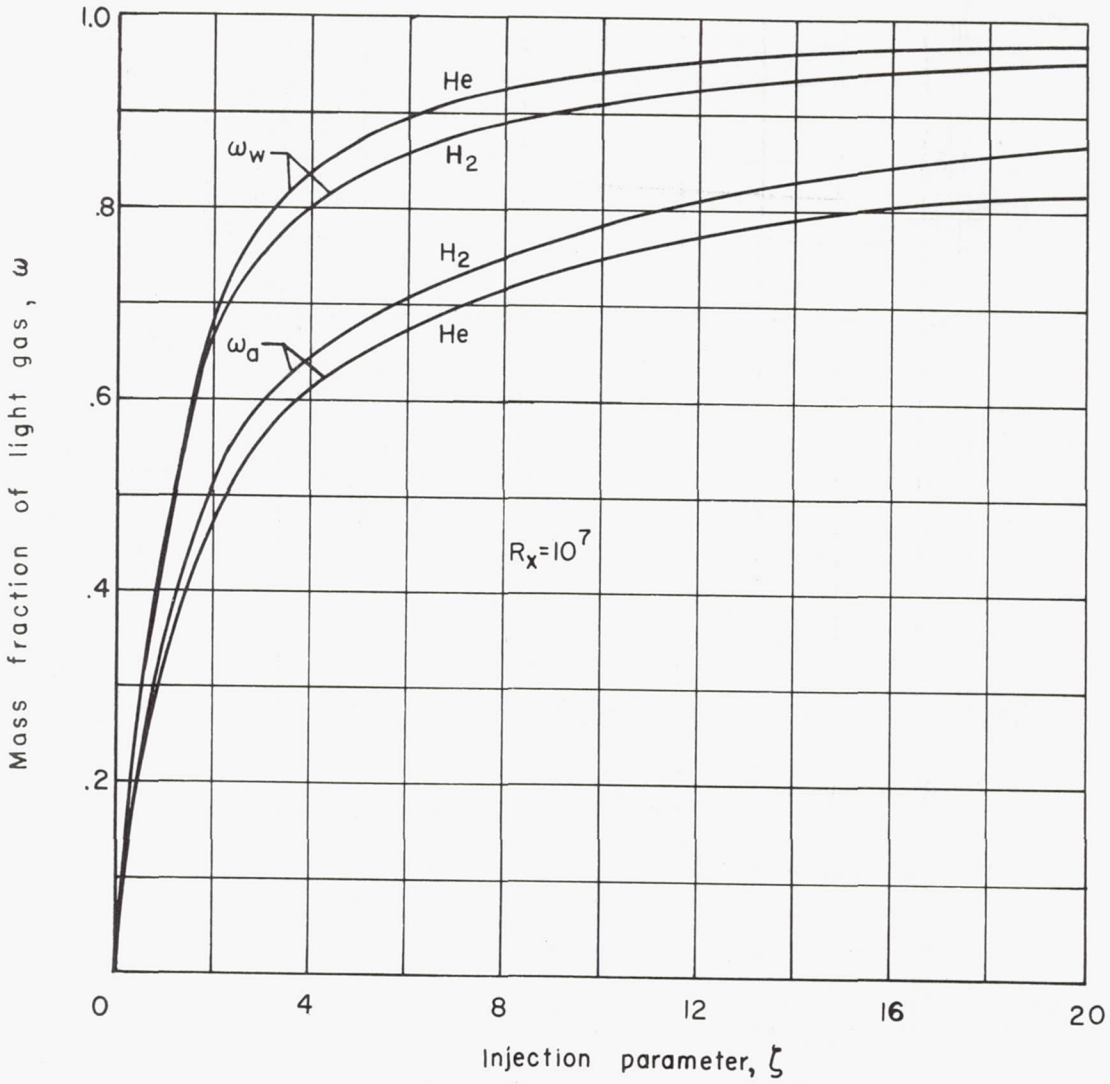

Figure 6.- Wall and interface light-gas concentration variation with dimensionless injection parameter.

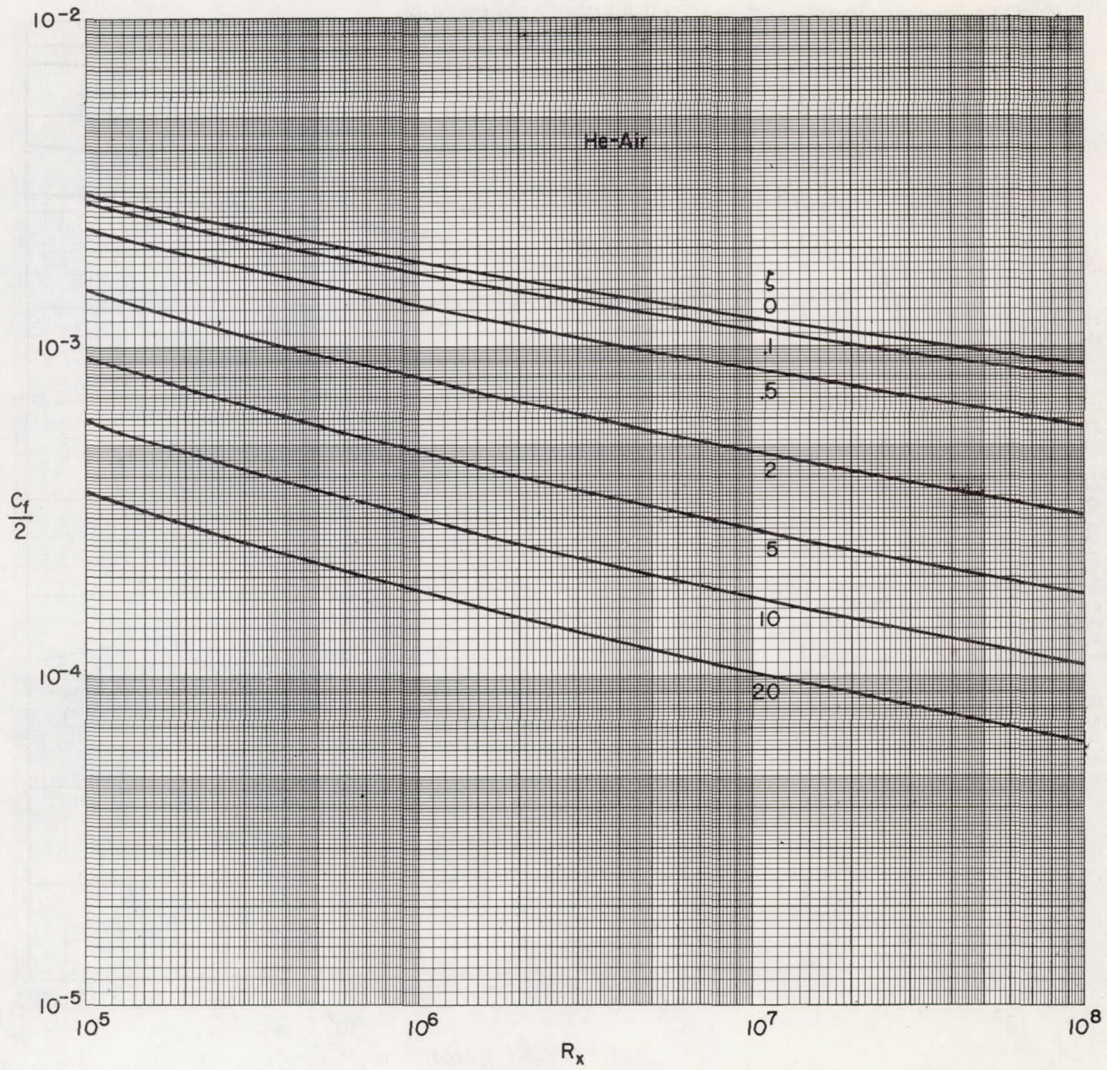

(a) He-Air

Figure 7.- Effect of distributed injection on local skin-friction coefficient.

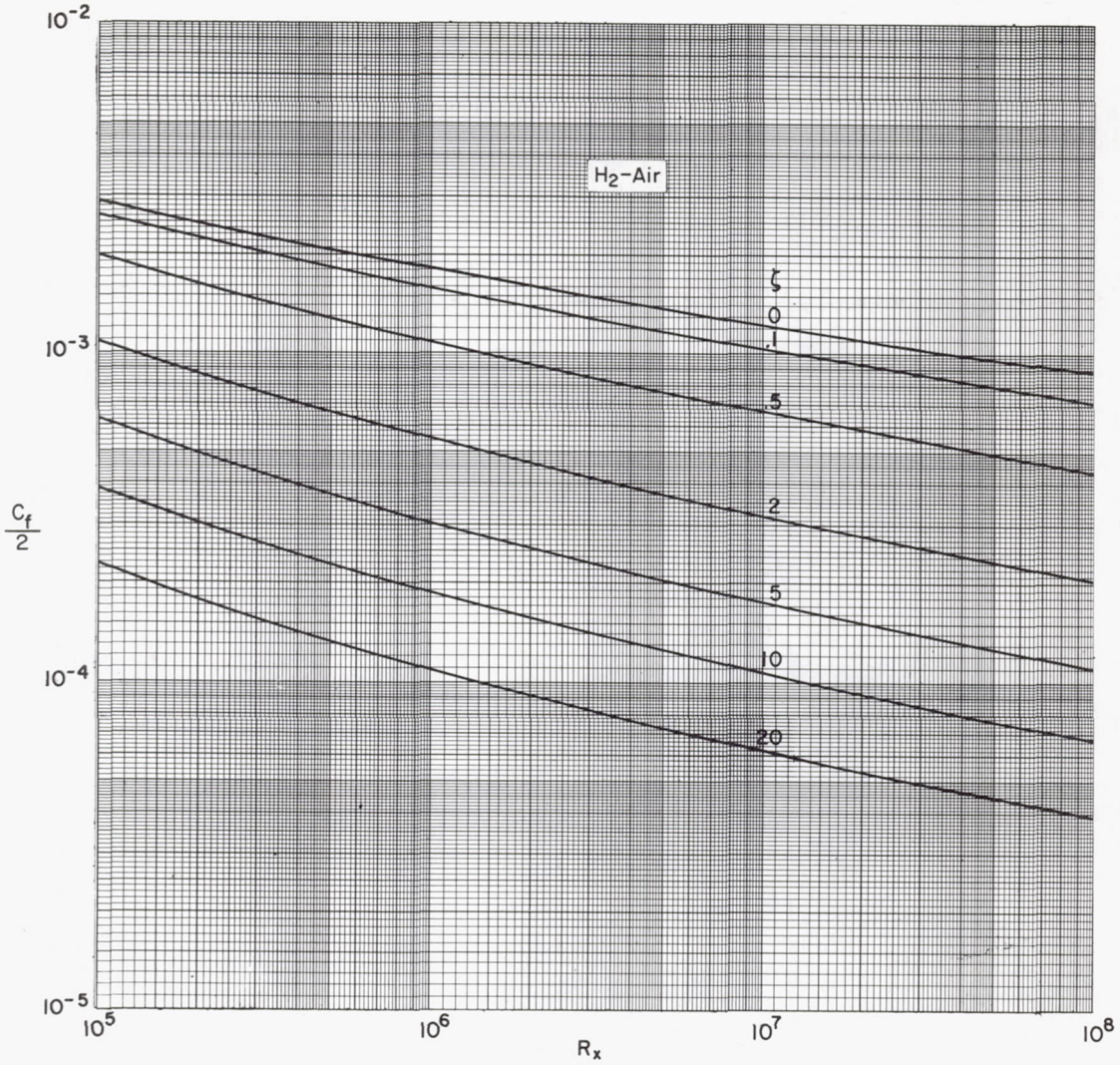

(b) H_2-Air

Figure 7.- Concluded.

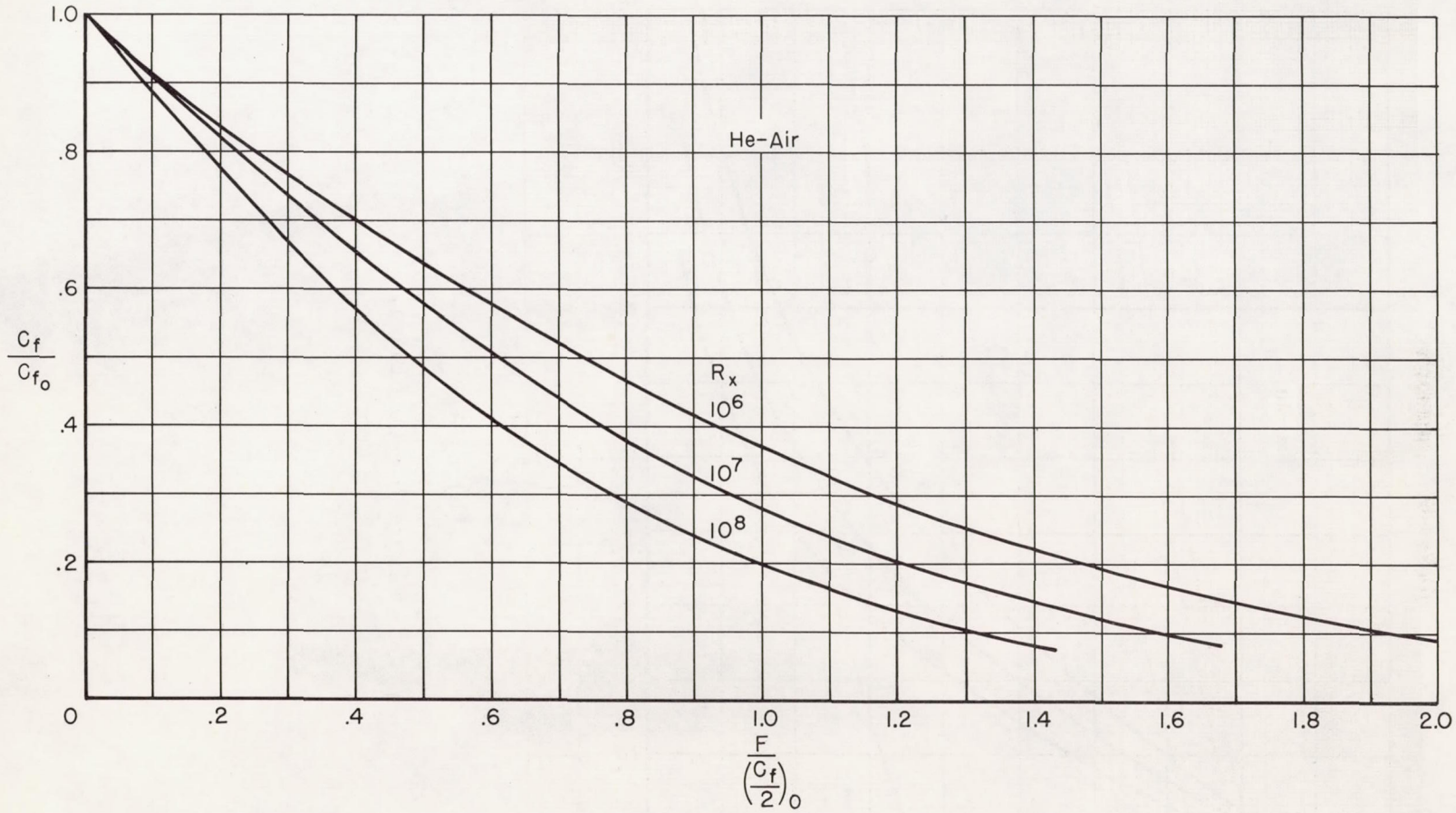

(a) He-Air

Figure 8.- Effect of distributed injection on skin friction.

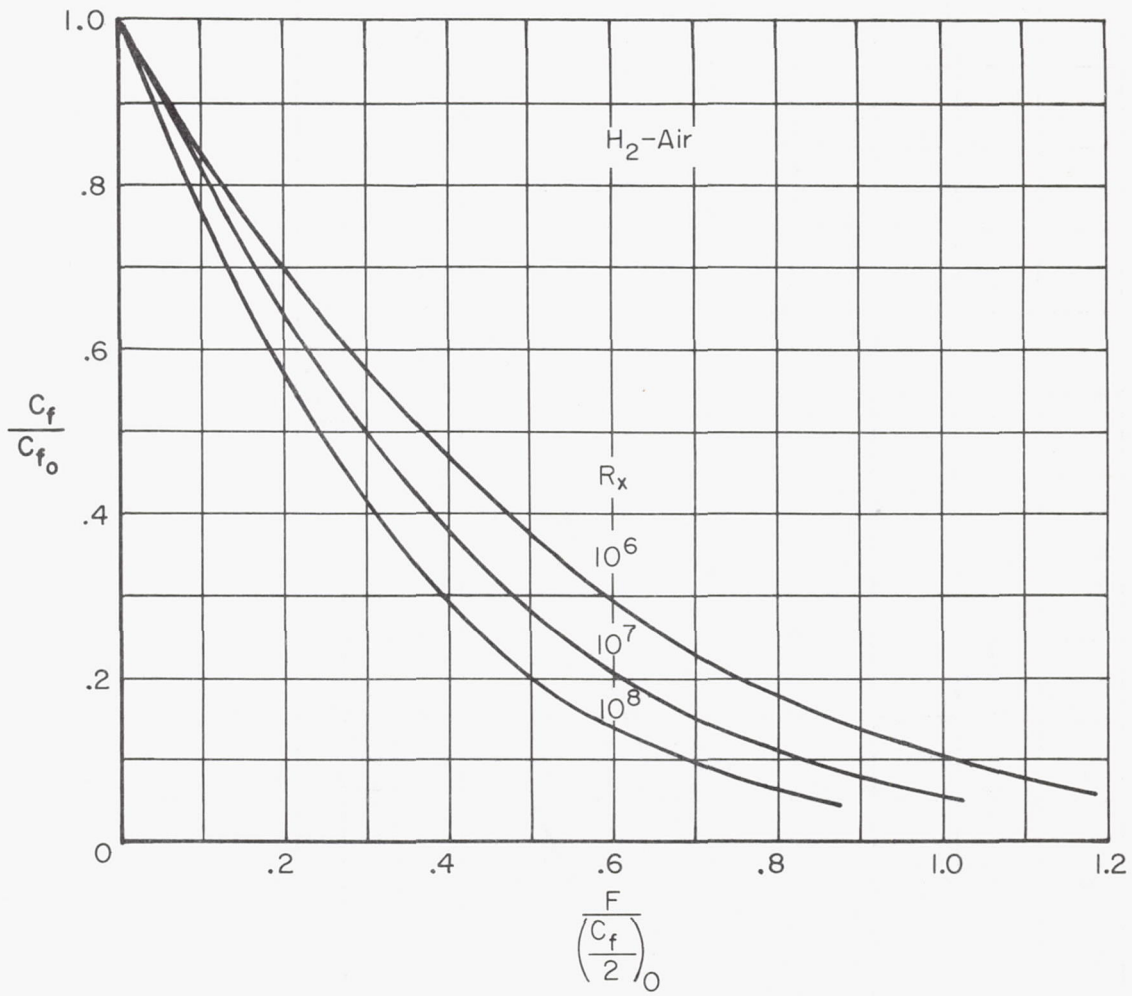

(b) H_2-Air

Figure 8.- Concluded.

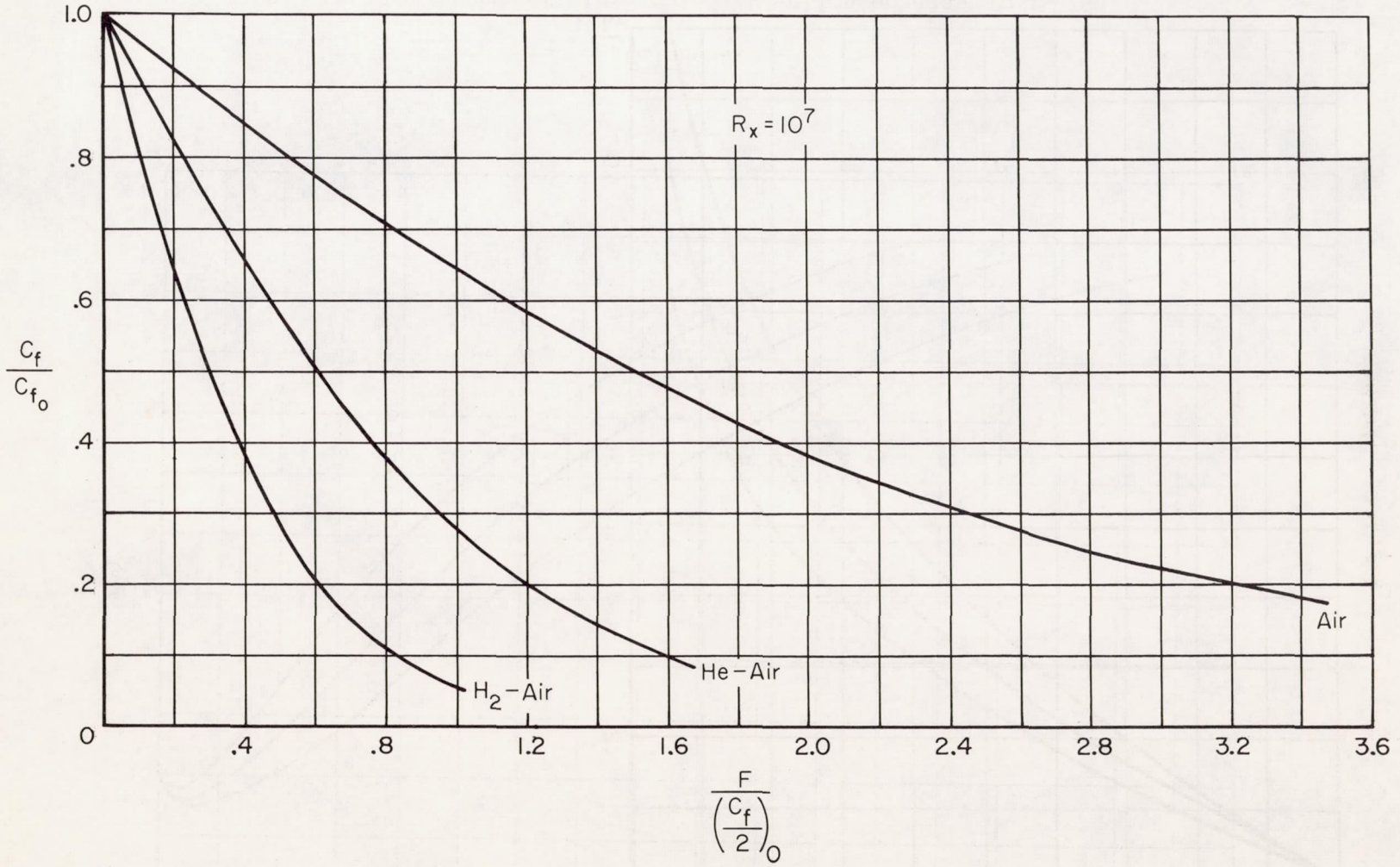

Figure 9.- Comparison of the effect of distributed injection of He, H_2, and Air on skin friction.

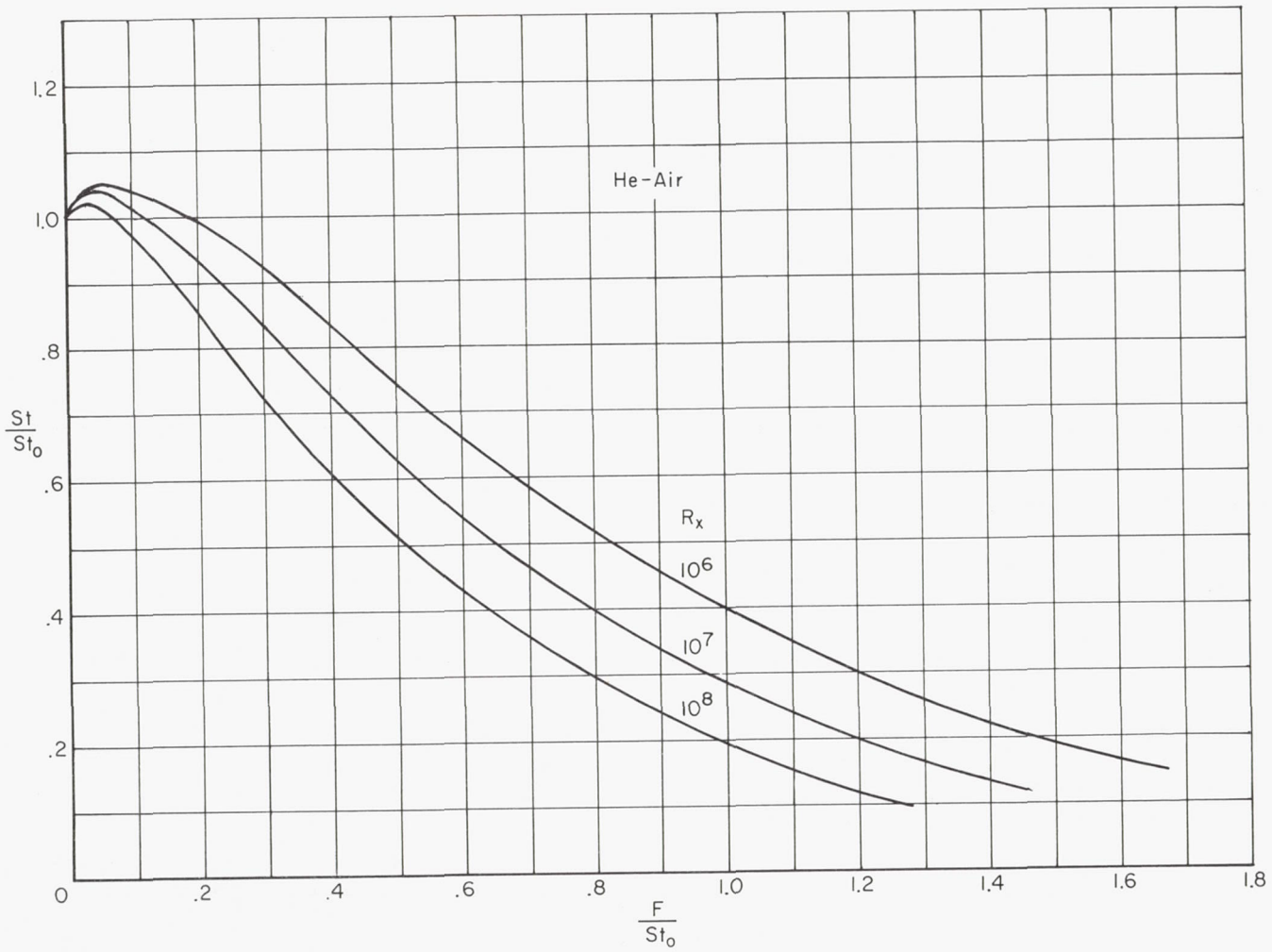

(a) He-Air

Figure 10.- Effect of distributed injection on heat transfer.

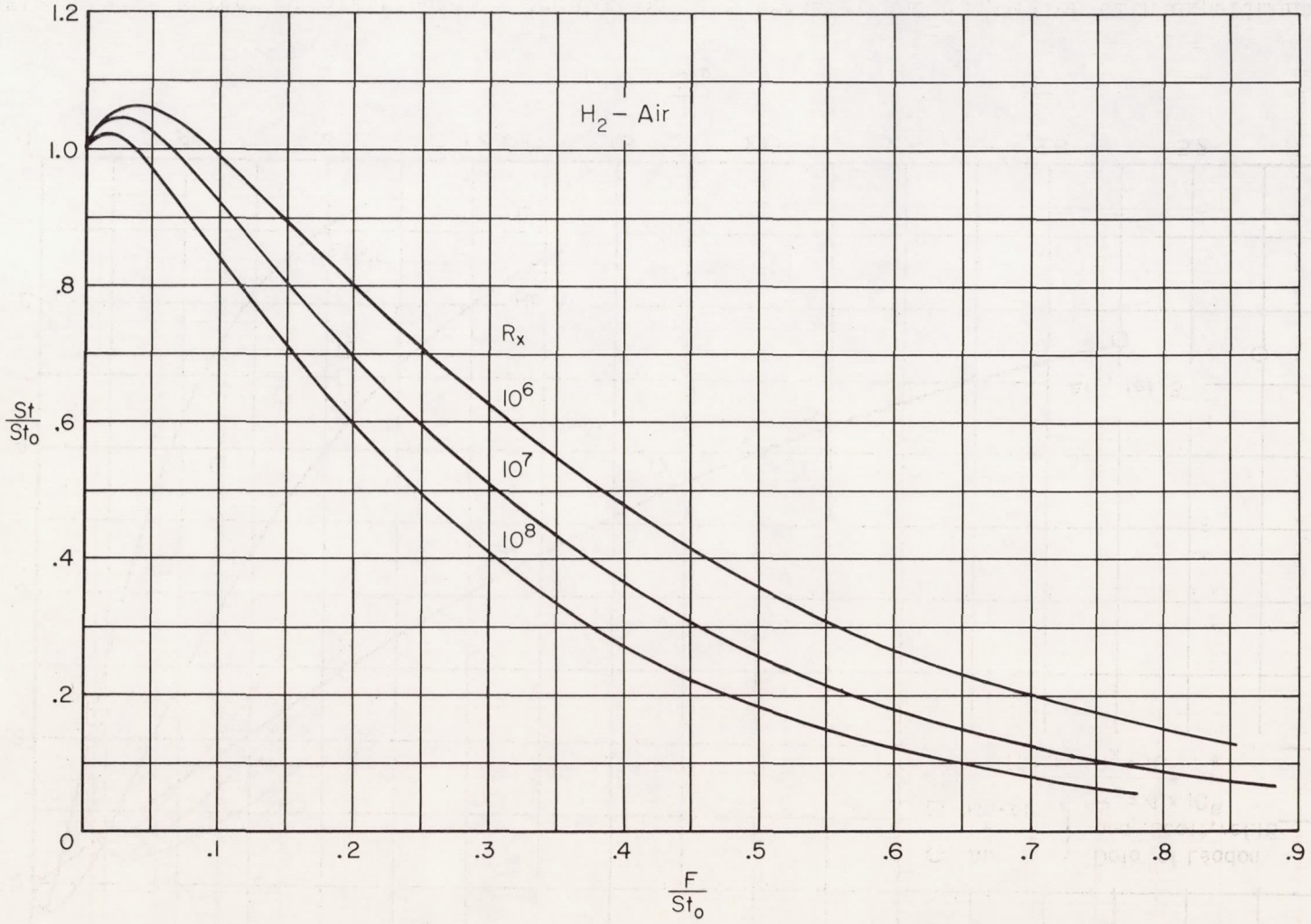

(b) H_2-Air

Figure 10.- Concluded.

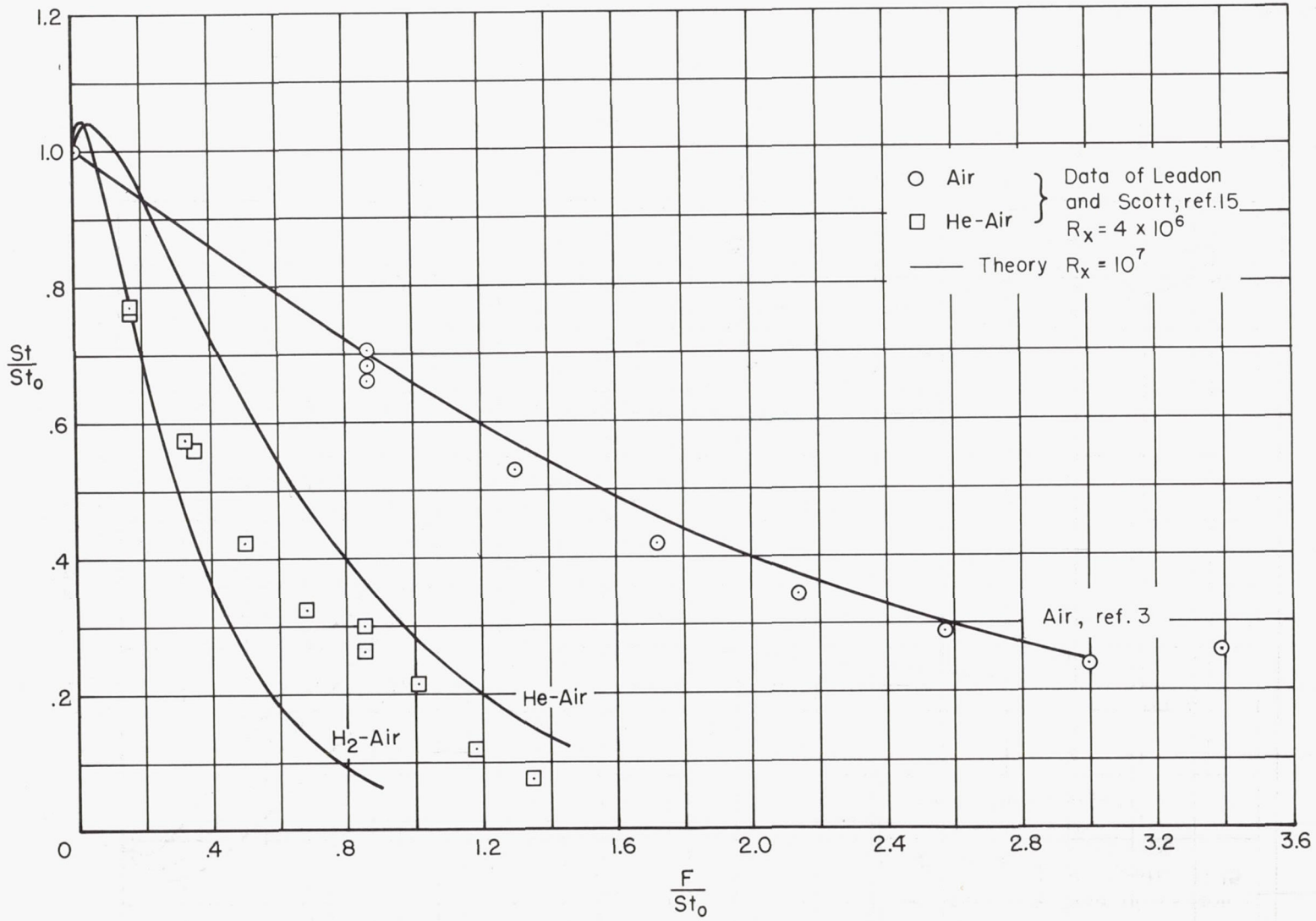

Figure 11.- Effect of distributed injection on heat transfer and comparison with experiment.

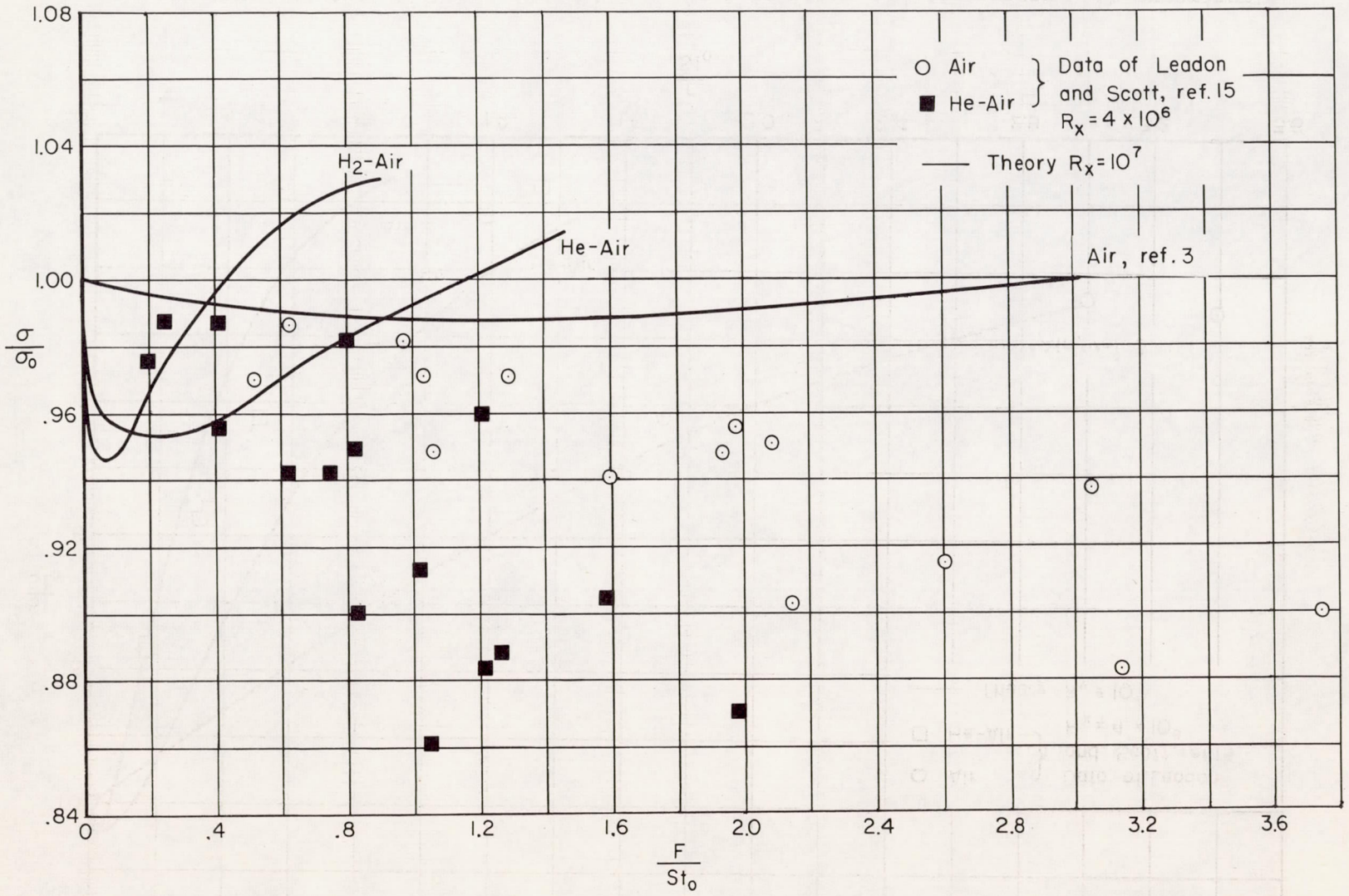

Figure 12.- Effect of distributed injection on recovery factor and comparison with experiment.

NACA - Langley Field, Va.